EXAMINATION OF THE MATERIAL REMOVAL RATE IN LAPPING POLYCRYSTALLINE DIAMOND COMPACTS

A Thesis

by

JASON MICHAEL SOWERS

Submitted to the Office of Graduate Studies of
Texas A&M University
in partial fulfillment of the requirements for the degree of

MASTER OF SCIENCE

August 2011

Major Subject: Mechanical Engineering

EXAMINATION OF THE MATERIAL REMOVAL RATE IN LAPPING POLYCRYSTALLINE DIAMOND COMPACTS

A Thesis

by

JASON MICHAEL SOWERS

Submitted to the Office of Graduate Studies of
Texas A&M University
in partial fulfillment of the requirements for the degree of

MASTER OF SCIENCE

Approved by:

Chair of Committee,	Hong Liang
Committee Members,	Gwo-Ping Fang
	Karl Hartwig
Head of Department,	Dennis O'Neal

August 2011

Major Subject: Mechanical Engineering

ABSTRACT

Examination of the Material Removal Rate in Lapping Polycrystalline Diamond Compacts. (August 2011)

Jason Michael Sowers, B.S., Texas A&M University

Chair of Advisory Committee: Dr. Hong Liang

This study examines the lapping machining process used during the manufacturing of polycrystalline diamond compacts (PDCs). More specifically, it is aimed at improving the productivity of the process by developing a better understanding of the parameters that affect the material removal rate (MRR) and MRR uniformity of lapped PDC samples.

Experiments that focused on several controllable lapping parameters were performed to determine to what extent they affected the process. It was determined that the MRR can be modeled with the Preston equation under certain ranges of pressure and speed. It was also found that using a hard and rigid sample holder produces higher MRRs than soft and flexible sample holders. The results have also shown that MRRs in excess of 300 μm per hour can be achieved while using 10 grams of diamond abrasive per PDC per hour of lapping. The productivity of the lapping process can also be improved by placing the maximum allowed PDC samples in a concentric circle on the edge of the sample holder. The MRR uniformity between samples lapped on the same sample holder was found to be dependent on the sample holder material.

This thesis is composed of six chapters. The first chapter introduces the need for PDC's as extreme cutting tools, the manufacturing process of PDC's, and the lapping process. The second chapter discusses the motivation behind this research and the primary objectives that were established. The third chapter details the materials and the experimental procedure, and the fourth chapter presents the results. The fifth chapter discusses the results, and the sixth chapter presents conclusions and information on possible future work.

ACKNOWLEDGEMENTS

I would first like to thank Dr. Alex Fang for his support, guidance, and encouragement throughout my graduate studies at Texas A&M University. I would also like to thank Dr. Hong Liang for her guidance and for allowing me to become a member of the Liang Research Group. I also thank Dr. Karl Hartwig and Dr. Richard Griffin for their support.

Thanks also to all of my friends and colleagues at Texas A&M University and within the Liang Research Group for supporting me and providing feedback throughout my studies. I also want to thank Texas A&M University and the entire Mechanical Engineering department for providing me with a top tier education.

Finally, I want to thank my family for their support throughout my entire education. To my Dad, for teaching me the importance of hard work and always being there to answer my math, physics, and engineering questions. To my brothers and sister, for their support. And to my Mom, for her constant love and representation of what it truly means to live for our Lord and Savior.

TABLE OF CONTENTS

Page

CHAPTER Page

Page

LIST OF FIGURES

Page

Page

Page

LIST OF TABLES

Page

Page

Page

CHAPTER I

INTRODUCTION

This chapter introduces the use of polycrystalline diamond compact drill bit inserts within the oil and gas industry. The lapping process, costs associated with lapping PDC's, and challenges associated with lapping PDC's are also discussed.

1.1. Polycrystalline Diamond Compacts

Polycrystalline diamond compacts (PDCs) were developed in 1964 and have since become known as exceptional cutting tools due to their extreme hardness, wear resistance, and isotropic behavior[1]. Today PDCs are most well-known for their use as drill bit inserts within the oil and gas industry, but they are also used as cutting tools for materials such as ceramics, polymers, wood, and non-ferrous metals[2-6].

PDCs are made in a high temperature and pressure sintering process and are composed of a tungsten carbide (WC) substrate, metal binder (usually cobalt), and polycrystalline diamond layer as shown in Figure 1[7]. Most PDCs manufactured are cylindrical in shape with diameters between 13 to 16mm and thickness of up to 14mm. The diamond thickness is typically between .5 and 2.5mm[7-9]. Starting from the late 1960's, PDCs have been used as drill bit inserts for operations around the world with much success, and there have been many reports on their wear resistance compared to other cutting tools used in the field[10-12]. Today PDC drill bits are responsible for 50% of the hole length drilled by the oil and gas industry in the world today[5].

This thesis follows the style of *Journal of Testing and Evaluation*.

The majority of research conducted on PDCs relates to the residual stresses during manufacturing. Due to the high temperatures seen during manufacturing and unequal thermal expansion coefficients of diamond and cobalt (1.18×10^{-6}/°C for diamond, 12.2×10^{-6}/°C for cobalt[13]), a significant amount of residual stress can develop when cooling[2, 9, 13]. In the early 1990's, Lin et al developed a model that showed compressive stresses above 1GPa may develop on the diamond layer, and tensile stresses up to 500MPa may develop in the tungsten carbide layer[9]. Since then, there have been several studies using micro-Raman spectroscopy or neutron diffraction to measure the residual stresses. The results from these tests are comparable to what was predicted by the developed model[2, 3, 13, 14]. Jia et al have shown that by reducing the mono-crystalline diamond size used in manufacturing the PDCs or the sintering temperature, the residual stresses can be decreased[3]. Recently, research was also conducted on using non-destructive test procedures to determine whether a produced PDC exhibits manufacturing flaws from the sintering process that would result in premature failure[8].

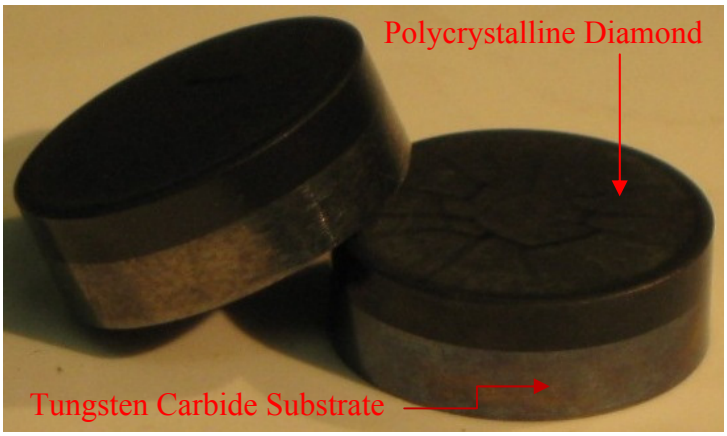

Figure 1. Polycrystalline Diamond Compact (PDC)[7]

1.1.1. Wear and Failure Mechanisms

The wear of PDCs can be classified into two categories depending on operating temperatures. At temperature of around 1000°C, which are can be seen during machining or drilling, chemical dissolution of the diamond is seen. That is, on an atomic level the PDC surface attaches to the material being cut and is carried away. This form of wear is not possible at lower temperatures, and the primary mode for wear is due to the formation and growth of micro-cracks[4]. Research has shown that improving the surface finish results in increases in wear resistance and strength[5].

1.1.2. Manufacturing PDCs for Drill Bit Inserts

1.1.2.1. Sintering Process

PDCs are manufactured through a sintering process using synthetic mono-crystalline diamond powders, a tungsten carbide substrate, and a metal binder. The metal binder used is usually Cobalt, however the use of other binder materials or no binder

material have also been studied[3]. Temperatures of 1400 to 2000 degrees Celsius and pressures of 5 to 7 GPa are seen during the process[2, 15].

1.1.2.2. Drill Bit Preparation

After sintering, PDCs must be machined to meet certain manufacturing requirements including thickness, flatness, and surface finish specifications. These requirements may vary depending on the manufacturing company and the type of drill bit being manufactured, but typically flatness and surface roughness (Ra) values less than 10 μm and 1 μm, respectively, must be obtained. The machining process used to meet these requirements is lapping, which is a similar machining process to polishing. The lapping process will be discussed in more detail in the following section.

The lapping process for PDCs can be grouped into two stages: roughing and finishing. During the initial roughing stage of lapping, the majority of the stock material that is required to be removed to meet thickness requirements is taken off. This process makes use of large abrasives (roughly 100 μm) to achieve high surface finishes. The finishing stage is then used to remove the remaining necessary stock material along with achieving the necessary surface finish and flatness requirements. Only recently has any research been conducted on the lapping process related to PDCs [7] as most companies classify this process as a trade secret. Through personal encounters, it has been established that lapping PDCs is an extremely costly process.

After the PDCs pass inspection, they are mounted to drill bits for operation by either being brazed or pressed into location[5].

1.1.2.3. Cost

A major cost associated with the manufacturing of PDCs is the surface finishing process because of the time it takes to complete and cost of diamond abrasives. Roughly 250 μm of stock material is removed during the lapping procedure, and the typical MRR seen industry is less than 100 μm per hour. During the time samples are being lapped, the process must be stopped about once an hour to sort PDCs into groups with similar thicknesses because of MRRs variances seen within lapped samples.

1.2. Lapping Process

Lapping is a machining process that has been used since the Stone Age when tools were worked using sand and a workpiece to achieve desired results[16]. Similarly to polishing, the lapping process has greatly improved over time and is currently used throughout industry to achieve fine surface finishes, flatnesses, and minimal subsurface damage where other machining processes fall short. In lapping, abrasives are supplied via an abrasive vehicle between the workpiece and tool, or lap plate. The mixture of abrasive and abrasive vehicle is referred to as slurry. The slurry can be applied continuously, a single time, or at time dependent rates. A load is applied to the workpiece, and the workpiece is moved over the lap plate.

Material removal during lapping is caused through both two and three-body abrasion [16-18]. In two-body abrasion, wear is caused by fixed abrasives or direct surface contact as shown in Figure 2a. This occurs in lapping when the abrasives embed into the lap plate which can be referred to as micro-cutting[16]. In three-body abrasion, abrasive particles are free to move between two surfaces (Figure 2b). The abrasives

move by either sliding or rolling between the workpiece and lap plate[16-18]. Many different machining setups are possible for lapping workpieces with different geometries[16]. A basic schematic for lapping a single side of a flat workpiece is shown in Figure 3. During the process the abrasives move into active positions between the workpiece and tool. There has been an extensive amount of research performed on two and three-body abrasion in areas including grinding, polishing, and chemical mechanical polishing (CMP)[19-32]. The results from these studies, along with research on lapping, can be used to help understand the lapping process.

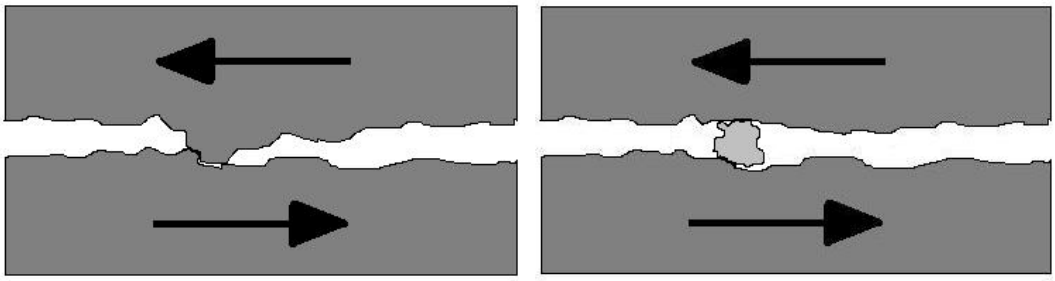

(a) (b)

Figure 2. Schematic of (a) Two-body abrasion (b) Three-body abrasion

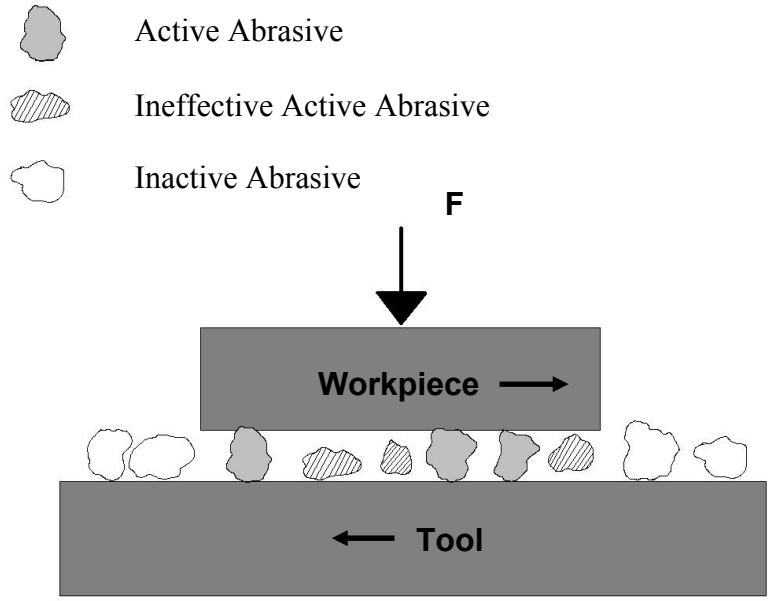

Figure 3. Schematic of single-sided flat lapping

1.2.1. Parameters Affecting the Lapping Process

1.2.1.1. Velocity and Pressure

In the 1920's, a model that related relative velocity and pressure to material removal rate (MRR) was established by Preston who was studying the effects of grinding glass[33]. This relationship, known as Preston's equation, is:

$$MRR = cPV \tag{1}$$

where c is a constant relating to the process parameters, P is the applied pressure, and V is the relative velocity of the workpeice on the tool. The constant parameter,c, changes based on any modifications to the material removal process such as abrasive type, abrasive vehicle, abrasive and vehicle feed rate, and other miscellaneous process parameters. Also important to note is that the MRR can be reported in different terms.

Most commonly MRR is reported in units of either density or thickness of material removed per unit of time. A c term that results in the desired unit system can then be established. The linear relationship in Preston's equation has stood true through numerous experiments conducted on forms of abrasive material removal at certain pressures and velocities[21, 26, 34-36]. However, when the model is applied to relatively high or low pressures and velocities, the relationship no longer holds true[19, 26, 27, 29, 37-39]. Pritchard has reported that the MRR is proportional to the applied load over a certain critical load[40]. It is generally accepted that the linear relationship shown in Preston's equation is no longer valid within certain ranges of lapping parameters[41]. In order to account for the differences seen between predicted and empirical results, there have been many proposed modifications to the Preston equation. Tellez-Arriaga et al have proposed a modification to Preston's equations which accounted for the frictional coefficient as a function of velocity at low speeds[37]. Several studies have used power functions in the form of

$$MRR = cP^nV^m \tag{2}$$

where n and m and variables that can be assigned based on the process[19, 27, 29]. There are also equations that have been developed specific to CMP processes that account for the chemical factor responsible for material removal[26]. In the end, all of the proposed equations are deviations from Preston's equation that result in better fits to empirical data collected from specific processes.

1.2.1.2. Abrasives

It has been established that abrasives play an important role on material removal based on size, shape, and hardness[17, 18, 31, 36, 42-44]. It has been shown that MRR increases with increasing abrasive size up to a critical size at which the MRR begins to stabilize and even decrease[18, 31, 41, 44]. There is a linear relationship between abrasive size and MRR up to the critical size, and MRR has also been reported to increase with increasing abrasive hardness[36, 43].

Multiple studies have also shown that surface roughness improves with decreasing grain size[35, 45-47]. Deshpande et al showed that flatness also improved during lapping with the use of smaller grain abrasives[47]. Lin et al showed that the MRR uniformity increases with decreased abrasive size[46]. The MRR has been shown to increase linearly with an increase in abrasive feed rates[18, 43]. Also, without a continuous supply of fresh abrasives to the lap plate, the MRR will decrease over time[48].

1.2.1.3. Abrasive Vehicle

The abrasive vehicle is the medium which transports the abrasive across the work piece. It is known that for abrasive material removal, the rheological properties of the abrasive vehicle are important to how effective the abrasives are in material removal[49]. It has been shown that increases to the abrasive vehicle viscosity result in greater MRRs to a critical point at which the MRR will decrease[41]. The decrease is believed to be due to the formation of a large fluid film between the workpiece and tool which limits the abrasives engagement[41]. Le et al have shown that spent slurry needs

to be removed from the lapping plate to allow other abrasives to be able to engage and work[39].

1.2.1.4. Kinematics

There has been a great amount of research conducted on the kinematics of lapping [21, 50-52]. Yuan et al have proposed using a relationship between the speed of the lap plate and workpeice to determine if the lap plate is worn uniformly[50]. Recently, a kinematic model has also been developed that relates specifically to the lapping process being studied in this research [53]. The average velocity of the PDC samples can be found from the equation

$$v_{mean}(\lambda, \kappa) = \omega_{plate} a_H \sqrt{1 + \kappa^2(\lambda - 1)^2} \tag{3}$$

where,

$$\kappa = \frac{\rho_H}{a_H}, \tag{4}$$

$$\lambda = \frac{\omega_{conditioning\ ring}}{\omega_{plate}}, \tag{5}$$

ω_{plate} is the lap plates rotational speed, a_H is the distance from the center of the lap plate to the center of the sample holder, ρ_H is the distance from the center of the sample holder to the center of the PDC, and $\omega_{conditioning\ ring}$ is the rotational speed of the sample holder in the conditioning ring. Figure 4 and Figure 5 show schematics of the lap plate and sample holder based on the kinematic model.

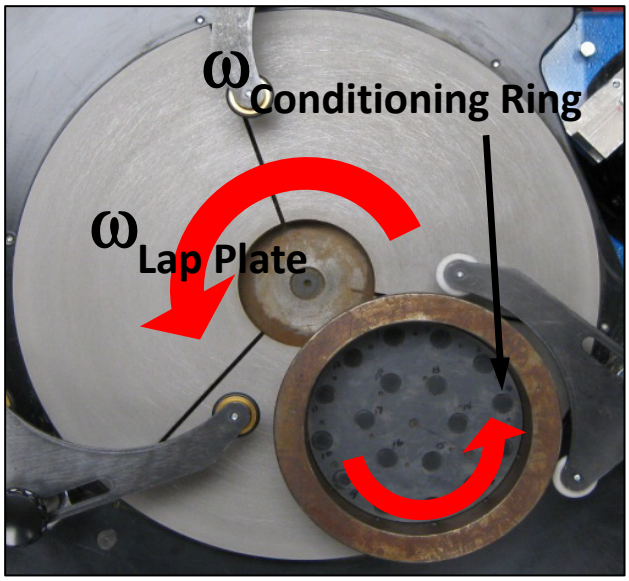

Figure 4. Schematic of the lap plate and conditioning ring locations

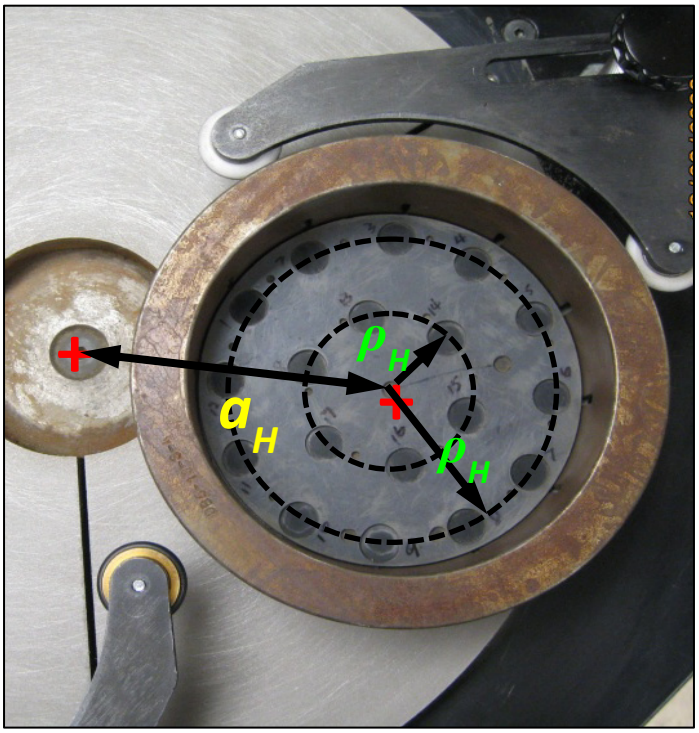

Figure 5. Schematic of where a_H and ρ_H are located

1.2.1.5. Prior Research

A couple studies have used acoustic emission (AE) to monitor material removal during abrasive wear[48, 54]. Using fixed abrasives, Sanchez et al have shown that the AE changes with changes in the workpiece surface roughness and MRR. Filho et al used non-replenishing slurry lap tests to characterize how pressure, velocity, and grain size relate to the AE. These techniques could be beneficial in monitoring PDC lapping during production to ensure the process does not encounter problems. Other research has shown that surface roughness decreases with increased speeds[31].

Previous research related to the same research being conducted in this study has looked into how accurate PDC lapping tests conducted over a 30 minute interval can represent lapping for 60 minutes. Both previously lapped and virgin samples were tested. The results from these tests are listed in Table 1, and they show that 30 minute tests are sufficient at modeling the process. Also, tests were conducted with three sample holders running at once on the lap plate to determine if using a single sample holder accurately represents the MRR that can be achieved while running three sample holders. The results from the tests are shown in Table 2 and show that running one sample holder is sufficient. These results are important from a research standpoint because material can be conserved.

Table 1. MRR results based on lapping tests conducted at different time intervals

PDC Sample Type	MRR (μm/hr) calculated based on lapping time				
	5 min	10 min	15 min	30 min	60 min
Previously Lapped PDCs	230	214	203	230	251
Virgin PDCs	-	-	-	274	288

Table 2. MRR results from tests with one and three sample holders

Experimental Setup	MRR (μm/hr)	
	Previously Lapped PDCs	Virgin PDCs
One Sample Holder	232, 227, 232 (Avg. = 230)	274
Three Sample Holders	273, 256, 187 (Avg. = 239)	309, 328, 299 (Avg. = 312)

CHAPTER II

MOTIVATION AND OBJECTIVES

The increased use of PDC's throughout industries has presented a need to develop a better understanding of the PDC manufacturing process. This research focuses on the lapping roughing stage within the manufacturing process and has three main objectives:

1. Establish a better comprehension of the lapping parameters that affect the MRR and increase the MRR.
2. Propose a general set of guidelines that can be used at any PDC manufacturing scale to reduce manufacturing costs.
3. Determine the major factors affecting the uniformity of the MRR within a set of lapped PDC's.

Since the lapping process is generally considered within most industries as a trade secret, there is little research that has been conducted that focuses on specific lapping manufacturing processes. Furthermore, there is even less understanding on the lapping process of PDC's due to the challenges associated with machining diamond. One of the major costs associated with lapping PDC's is time. Determining the factors that affect the MRR and uniformity during the roughing stage of PDC manufacturing is crucial to reducing costs through productivity and material use. With these better understandings, a set of guidelines can be established specifically for the process of lapping PDC's.

To complete the objectives a series of experimental tests will be performed to see how common parameters relate to the MRR of PDC's. Two main focuses will be on establishing the relationship between the lapping pressure and velocity to the MRR, which are two well know parameters that affect the MRR during lapping. Several more not as obvious parameters will also be tested including the: abrasive vehicle, size and concentration of abrasives, abrasive application rate, PDC holder design and layout, and the lap plate type.

CHAPTER III

EXPERIMENTAL

This chapter focuses on the experimental procedures that were taken to complete the research objectives. First, the type and description of the materials will be given. Next, the sample and test preparations will be discussed, and lastly, the experimental procedure and data collection will be outlined.

3.1. Materials

The PDCs used for this research were obtained through a company that manufactures PDCs and PDC drill bits. The PDCs were manufactured through a high temperature and pressure sintering process using synthetic diamond powder, a cobalt binder material, and tungsten carbide substrate as described in the Introduction section. The samples were round shaped with a diameter of 13 mm. Both virgin (never lapped) and lapped PDC samples were obtained. Table 3 lists several generic PDC properties that have been obtained through speaking with manufacturing companies. It is important to note however that PDC properties can vary from different manufacturers due to process parameters.

The abrasives used were bulky shaped synthetic mono-crystalline diamond abrasives purchased through DIN Diamond suppliers. The abrasives were 140/170 mesh (≈ 100 μm).

Table 3. Polycrystalline diamond compact properties

Shape	cylindrical (can also be cuboidal or cut to other shapes)
Diameter (mm)	13, 16 (other sizes can also be manufactured)
Diamond Thickness (mm)	2 (other thicknesses possible)
Tungsten Carbide Thickness (mm)	4 to 16
Sintering Temperature (°C)	1200 to 1300
Sintering Pressure (GPa)	8.6
Cobalt Composition (%)	3 to 6

3.2. Sample and Test Preparation

3.2.1. PDC Preparation

If necessary due to rough surfaces, the tungsten carbide side of the samples were lapped using silicon carbide abrasives. The PDC samples thicknesses were then measured using a Mitutoyo digital micrometer and sorted into groups of similar thicknesses within about 75 μm (3 mils). Samples being lapped together within a group on a sample holder were then labeled numerically (see Figure 6a) using an ARKOGRAPH A 50/6 electric arc metal engraver. Before each test, the samples in a group had their thicknesses measured and recorded at five locations on the PDC using the micrometer (see Figure 6b).

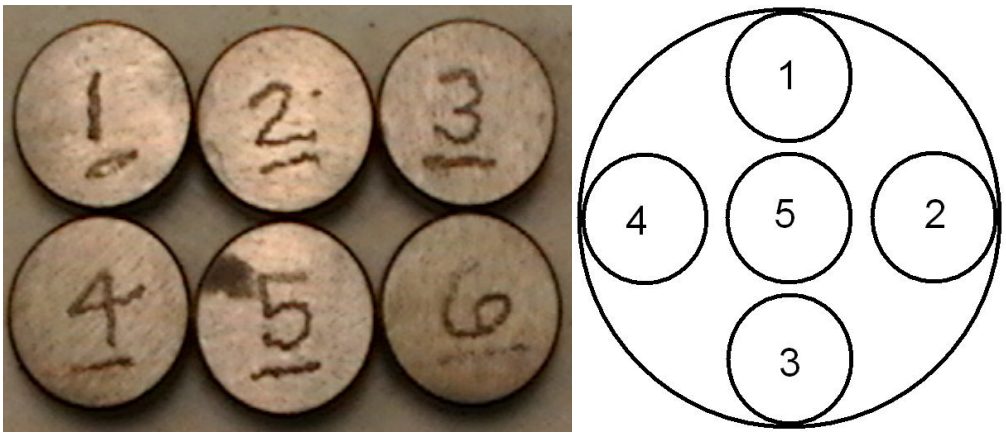

(a) (b)

Figure 6. (a) Labeled PDCs (b) Thickness measurement locations

3.2.2. Suspension Vehicle Preparation

The first step in preparing the lapping suspension vehicle is making a 1% concentrated gel solution of the carbomer polymer. This was accomplished by adding 30 g carbomer with 3 L DI water. The solution was shaken for several minutes and then allowed to sit for a day. The gel was shaken again and allowed to sit again and this process was repeated several times until the carbomer was fully wet.

Next, the 1% carbomer premix gel base was mixed with DI water and Triethanolamine (TEA) using a low shear rate stirrer. The Depending on the carbomer concentration of the vehicle being made, different amounts of each material were added. The two carbomer vehicle concentrations produced for this research are listed below in Table 4.

Table 4. Vehicle carbomer concentration chart

Vehicle Carbomer Concentration (%)	1% Carbomer Premix Gel (mL)	DI Water (mL)	Tea (mL)
0.111	400	3200	25.6
0.133	400	2600	25.6

3.2.3. Specimen Holder Preparation

3.2.3.1. Rubber Sample Holders

The rubber specimen holders used in this experiment were manually made. They consist of a rubber backing material that has one side come in contact with the tungsten carbide side of the PDC samples and the other side contacts the weight added during lapping. The type of rubber was changed during different lapping tests. The other side of the specimen holder is glued to the rubber backing with epoxy. It is a thermoset polymer that has holes cut into it that are roughly the diameter of the PDCs. Its function is to hold the PDCs in place during lapping, and it is thinner than the PDCs so it does not contact the lap plate during testing (see Figure 7).

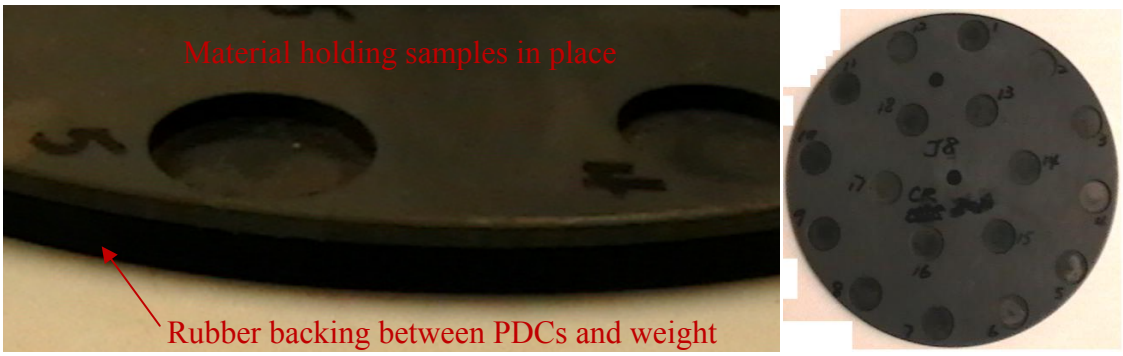

(a) (b)

Figure 7. (a) Image of the rubber sample holder cross section (b) Image of the location PDCs are placed on the rubber sample holder

3.2.3.2. Stainless Steel Sample Holder

The stainless steel sample holder is a solid cylindrical piece of (insert grade) that is 6.38mm thick. The surface of the plate was cleaned with acetone before each test to remove any debris from previous tests. Using a template, the plate was labeled with a permanent marker to designate the location of where the samples needed to be placed (see Figure 8a). Double sided tape produced by 3M was then applied to the surface of the plate where samples were to be placed (see Figure 8b). The PDC samples were then attached to the tape.

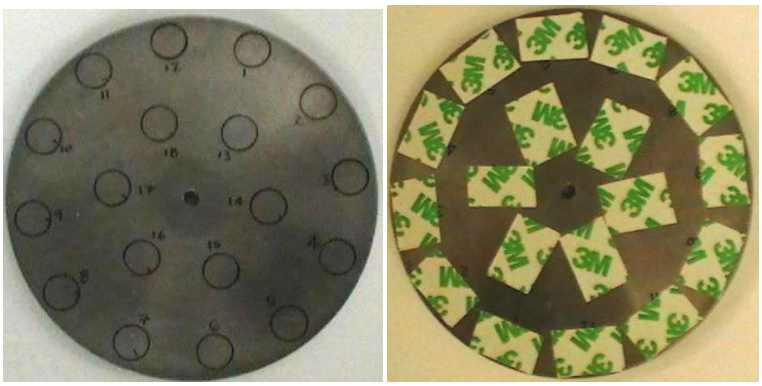

(a) (b)

Figure 8. Stainless steel sample holder with (a) PDC locations drawn on (b) double-sided sticky tape

3.2.4. Lapping Machine Preparation

The lapping machine used for experimentation was a LAPMASTER 15. The machine is equipped with a variable speed control for speeds up to 120 RPM. The lap plate used during experimentation was a 15 inch cast iron plate with 12 segments as shown in Figure 9. The lapping plate was monitored for flatness throughout experimentation using a flatness gage. As necessary the plate was reconditioned using either diamond or silicon carbide abrasive slurries. During reconditioning, 3 weighted conditioning rings were positioned on locations depending on the concave or convex profile of the lap plate.

Two conditioning ring roller arms were positioned on the lapping machine. One was located for a conditioning ring that was used to distribute the slurry (no samples were loaded inside), and the other for the conditioning ring that housed the samples. A

peristaltic pump was set up to deliver the abrasive slurry to the lap plate. The pump was calibrated to deliver the slurry at the desired rate. The hose was positioned and secured on a conditioning ring roller arm so that the slurry was delivered towards the inside of the lap plate in front of the condition ring as shown in Figure 10.

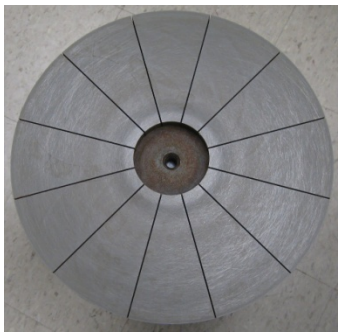

Figure 9. 12 slot segmented cast iron lap plate.

(a) (b)

Figure 10. Positioning of (a) conditioning rings (b) the peristaltic pump hose for slurry delivery

3.3. Lapping Procedure

The steps involved for loading the samples prior to testing include:

1. Manually applying abrasive slurry to the lap plate until the plate is fully wet (Figure 11a).
2. Loading the condition ring responsible for distributing slurry. Run lap plate with slurry being delivered for 30 seconds and set lap plate speed to desired speed (Figure 11b).
3. Loading the sample conditioning ring and samples (with no weight) and running lap plate with slurry being delivered for 30 seconds (Figure 11c).
4. Loading the weight on the sample holder. The weight varies based on the desired lapping pressure which is calculated by the surface area and number of PDCs (Figure 11d).

After the weight is applied the lap plate and slurry delivery are turned on and run for 30 minutes. During the lapping procedure the machine is monitored to ensure the lapping process stays consistent by monitoring the lap plate speed and abrasive delivery. Also, the speed of the conditioning ring that houses the samples is monitored and recorded periodically using a CHECK-LINE digital tachometer.

One lapping experiment involves using water as the lapping fluid. For this type of abrasive vehicle, diamond particles will not suspend and a different method for applying the abrasives is necessary. This process includes sorting the diamond abrasives into groups that can manually be applied at given time intervals based on the target

abrasive consumption rate, and using the peristaltic pump to deliver water to the lap plate at the desired rate.

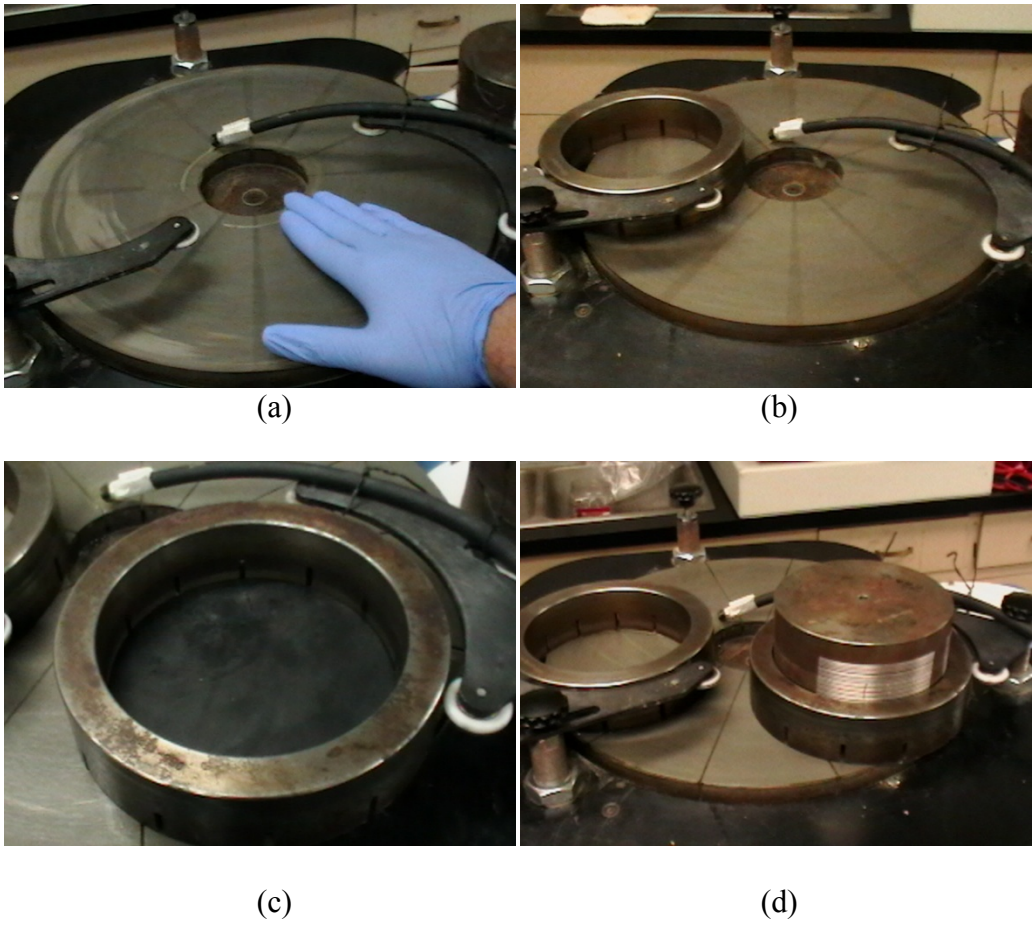

(a) (b)

(c) (d)

Figure 11. (a) Manual application of abrasive slurry (b) evenly distributing abrasive slurry (c) loading of condition ring and samples (d) loading of weight

3.3.1. Collection of Used Abrasive

The lapping sludge was collected from several tests by:

1) Prior to testing, the lap plate was removed from the lap machine and debris in the drainage well from previous tests was removed.
2) A container large enough for collecting sludge from a 30 minute lap was placed under the drainage channel (Figure 12a).
3) After completion of lapping, the sludge on top of the lap plate was sprayed into the drainage well with DI water.
4) The lap plate was removed and sludge was transferred into the container (Figure 12b).

(a) (b)

Figure 12. (a) Collection of sludge from lap test (b) Drainage well and sludge collection

3.3.2. Post-lap Procedure

After testing, the PDC samples were removed from the sample holder. A putty knife was forced under the PDC to pry it off the tape for samples on the steel holder. The samples were then washed with water and the surfaces were cleaned with acetone. The thicknesses of the PDC samples were then measured and recorded as described above (Figure 6b). The PDC samples were then visually inspected for any irregularities in appearance.

3.4. Characterization

3.4.1. Optical Microscope

PDC samples, collected sludge, and cleaned diamond abrasives were all examined using optical microscopy. A Keyence VHX-600 digital microscope was used in combination with Keyence VH-Z20 and VH-Z200 lenses to take images at different magnifications.

3.4.2. Scanning Electron Microscope

The surfaces of lapped PDCs were examined under high magnification using a JEOL JSM-6400. The SEM was operated between 5 and 15kV at working distances and magnifications between 10 to 11mm and 500 to 10,000X, respectively.

3.5. Roughness Measurements

Roughness measurements of the lapped PDC samples were made after various lapping tests were performed. The tests were conducted with a Mitutoyo SURFTEST 301 surface tester.

3.6. Calculations and Data Analysis

The material removal rate at each measurement location was calculated by

$$MRR = 2 \times (t_i - t_f) \tag{6}$$

where t_i and t_f are the initial and final recorded thicknesses, respectively. The difference in thickness is multiplied by a factor of two because each lapping test was conducted over a 30 minute time interval, and the standard in industry for reporting MRR is in μm of thickness removed per hour. For each lapping test using individual PDC MRRs, averages and standard deviations were calculated among all samples lapped together and samples that were arranged concentrically in the sample holder. The average PDC relative velocity, v_m, was calculated with Equation 3.

JMP data analysis software was used to analyze the MRR results. A Tukey-Kramer analysis was used to make pair-wise comparisons between tests that were performed to determine whether or not the MRRs were statistically different from one another. Also, quantile and histogram plots were made to look at the MRR distribution between samples on the same sample holder.

CHAPTER IV

EVALUATION OF MATERIAL REMOVAL RATE

This chapter presents the results obtained from the lapping tests that were explained in the previous chapter. First, the effects of different lapping parameters on the MRR will be given. Next, results on the surface analysis of the PDC and reclaimed diamond abrasives will be presented.

4.1. Effects of Lapping Parameters on MRR

4.1.1. Pressure and Speed

The effects of pressure and speed on the MRR of lapped PDCs were evaluated through a series of tests conducted at four different pressures and two different lap plate speeds. Each test was conducted while holding all other lapping parameters constant which are shown in Table 5. The results from tests lapped at 60 RPM and 96 RPM are shown in Figure 13 and Figure 14, respectively. Note that the 'Outer Ring' refers to the 12 samples concentrically placed towards the outer perimeter of the sample holder whereas the 'Inner Ring' corresponds to the 6 samples placed towards the middle of the sample holder. It can be seen that at lap plate speeds of 60 RPM, the MRR increases with increased pressure. At speeds of 96 RPM, the effects of pressure are not as substantial at pressures between 33 and 56 KPa. All error bars listed represent the MRR standard deviations. Table 6 and Table 7 show the p-values from a Tukey-Kramer HSD test at a 95% confidence level comparing the MRRs from the tests at 60 and 96 RPM, respectively. From the results it can be seen that at 60 RPM all the tests at different

pressures have significantly different MRRs, and at 96 RPM the test at 13.44 KPa has a significantly different MRR then at the other tested pressures. A more detailed discussion on the uniformity of lapped samples is discussed later. Additionally, the average recorded specimen holder ring speed during each test is reported in Figure 15. It is seen that at lower pressures the sample holder speed is increased when the lap plate speed is increased whereas at higher pressures the difference is not as substantial.

Table 5. Lapping parameters for results shown in Figure 13 and Figure 14

Number of PDC Samples	18
Specimen Holder Material	Stainless Steel
PDC Layout Pattern	2-Ring
Abrasives	14/170 mesh mono-crystalline diamonds
Vehicle Abrasive Concentration (g/L)	75
Vehicle Carbomer Concentration (%)	0.133
Vehicle Delivery Rate (L/min)	30

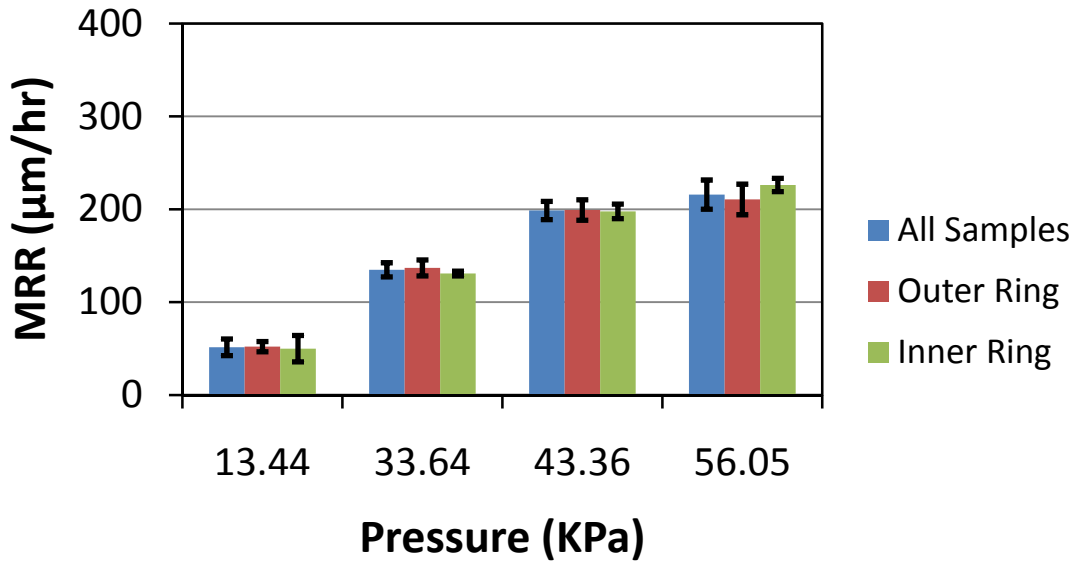

Figure 13. Results from lapping with lap plate at 60 RPM. Test parameters are in Table 5.

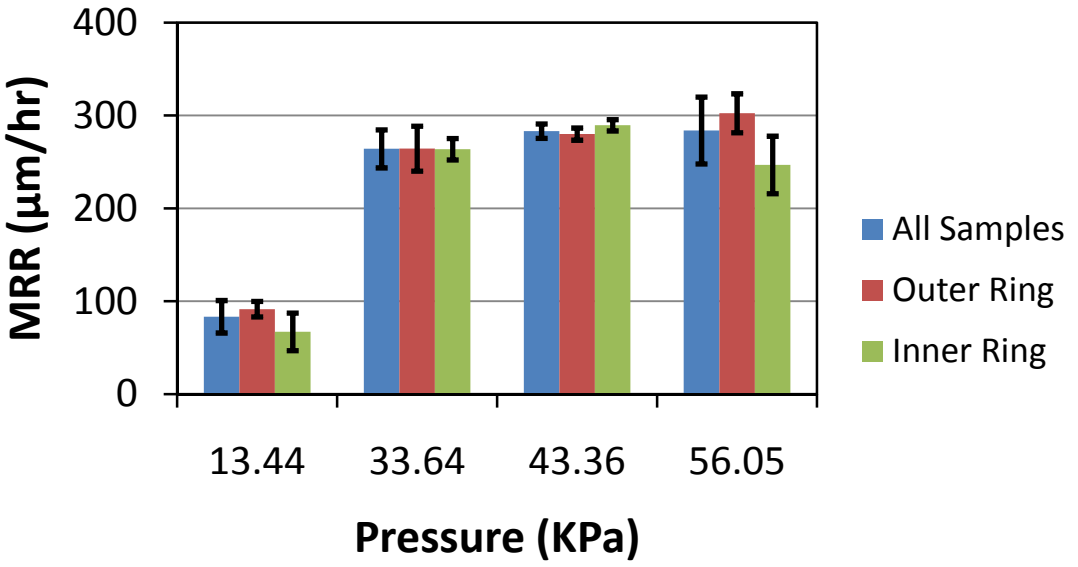

Figure 14. Results from lapping with lap plate at 96 RPM. Test parameters are in Table 5

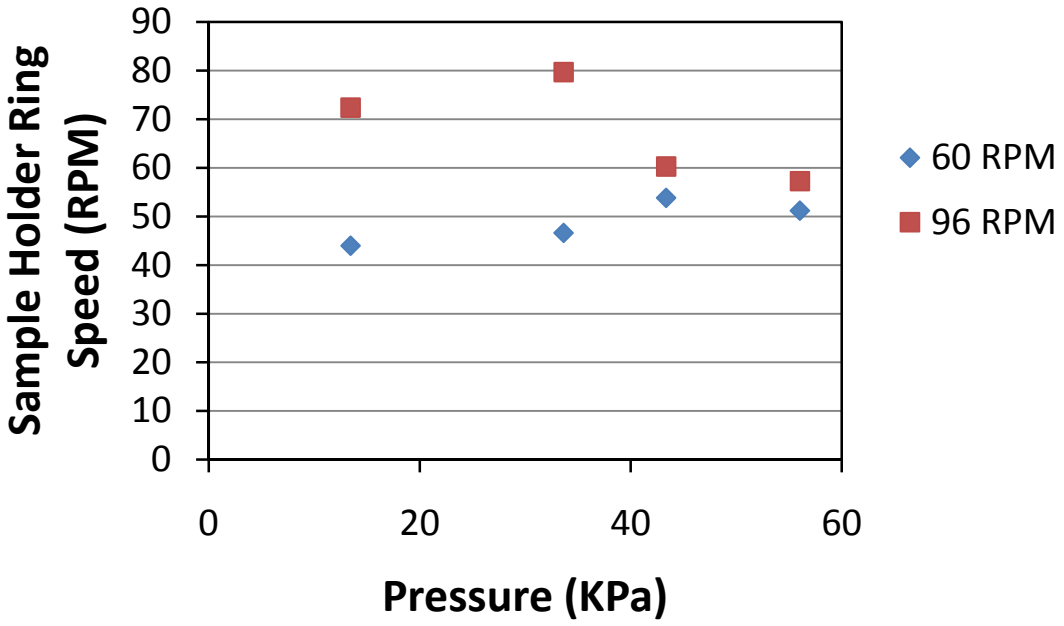

Figure 15. Observed sample holder ring speed as a function of pressure and lap plate speed

Table 6. Tukey-Kramer HSD test p-values at 95% confidence level for results from Figure 13. Pressures not connected by a bold p-value represent MRRs that are significantly different

Pressure (KPa)	13.44	29.58	43.36	56.05
13.44	-	< 0.0001	< 0.0001	< 0.0001
29.58	< 0.0001	-	< 0.0001	< 0.0001
43.36	< 0.0001	< 0.0001	-	< 0.0001
56.05	< 0.0001	< 0.0001	< 0.0001	-

Table 7. Tukey-Kramer HSD test p-values at 95% confidence level for results from Figure 14. Pressures not connected by a bold p-value represent MRRs that are significantly different

Pressure (KPa)	13.44	29.58	43.36	56.05
13.44	-	< 0.0001	< 0.0001	< 0.0001
29.58	< 0.0001	-	***0.0680***	***0.0550***
43.36	< 0.0001	***0.0680***	-	***0.9997***
56.05	< 0.0001	***0.0550***	***0.9997***	-

4.1.2. Abrasive Delivery Rate

Two sets of experiments were performed to determine the effect the abrasive delivery rate had on the MRR. The first set of tests involved varying the vehicle abrasive concentration while holding the vehicle delivery rate constant. The parameters from these tests are shown in Table 8 and the results in Figure 16. It can be seen that the MRR increases linearly with an increase in the abrasive delivery rate up to a critical point at which no more increases are seen. The second set of tests held the vehicle abrasive concentration the same and varied the vehicle delivery rate. The parameters from the tests are shown in Table 9 and the results in Figure 17.

Table 8. Test parameters for results shown in Figure 16

Number of PDC Samples	18
Specimen Holder Material	Stainless Steel
PDC Layout Pattern	2-Ring
Abrasives	14/170 mesh mono-crystalline diamonds
Lap Plate Speed (RPM)	96
Pressure (KPa)	43.36
Vehicle Carbomer Concentration (%)	0.133
Vehicle Delivery Rate (L/min)	30

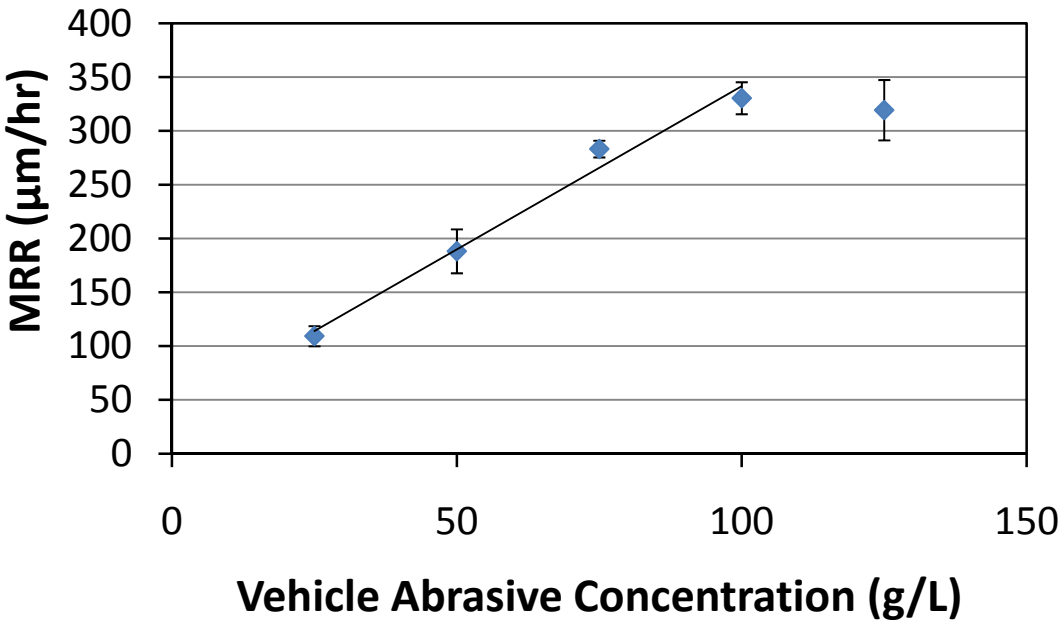

Figure 16. MRR results at varying vehicle abrasive concentrations. Test parameters are in Table 8.

Table 9. Test parameters for results shown in Figure 17

Number of PDC Samples	18
Specimen Holder Material	Stainless Steel
PDC Layout Pattern	2-Ring
Abrasives	14/170 mesh mono-crystalline diamonds
Lap Plate Speed (RPM)	96
Pressure (KPa)	43.36
Vehicle Abrasive Concentration (g/L)	75
Vehicle Carbomer Concentration (%)	0.133

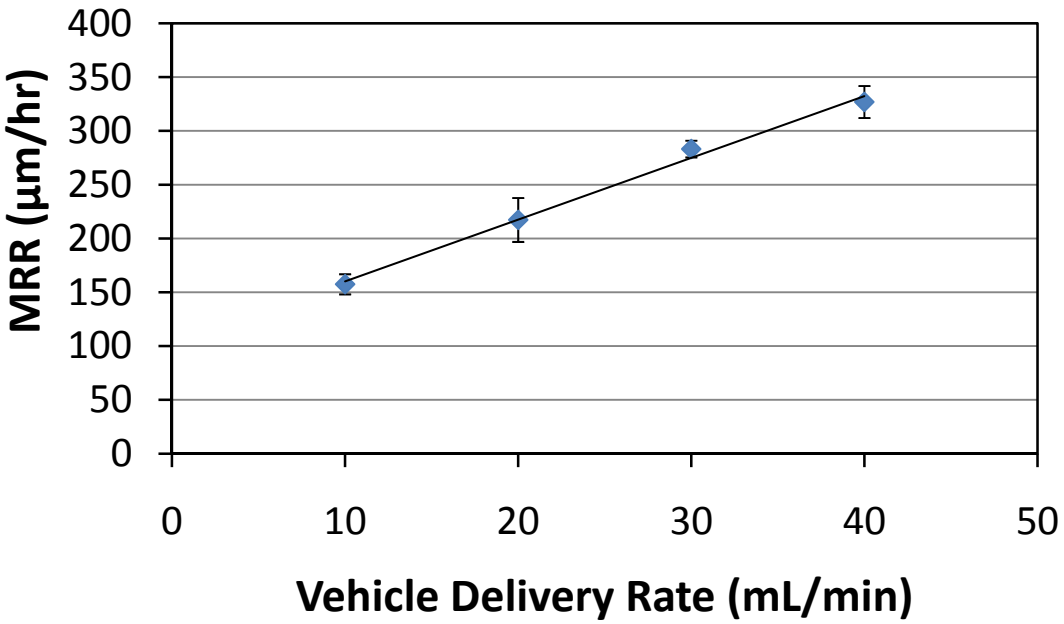

Figure 17. MRR results are varying vehicle delivery rates. Test parameters are in Table 9.

4.1.3. Vehicle Carbomer Concentration

A series of six tests were conducted to see the effect vehicle carbomer concentration had on MRR. The tests were conducted with two different vehicle carbomer concentrations (0.111 and 0.133 %) with three different abrasive concentrations (75, 100, and 125 g/L). The parameters held constant during testing are listed below in Table 10. The results from these tests are shown in Figure 18. Table 11 shows the p-values that show how the MRRs from the different tests relate to one another. These results show that while using a vehicle carbomer concentration of 0.111%, the MRR increases at abrasive concentrations of 75 to 100 g/L and decreases from 100 to 125 g/L. With vehicle carbomer concentrations of 0.133%, the MRR decreases at abrasive concentrations from 75 to 125 g/L. Also, at abrasive concentrations of 100 and 125 g/L, the 0.111% carbomer abrasive vehicle produces higher MRRs than the 0.133% carbomer vehicle.

Table 10. Lapping parameters for results shown in Figure 18

Number of PDC Samples	18
Specimen Holder Material	Stainless Steel
PDC Layout Pattern	2-Ring
Abrasives	14/170 mesh mono-crystalline diamonds
Lap Plate Speed (RPM)	96
Pressure (KPa)	43.36
Vehicle Delivery Rate (L/min)	30

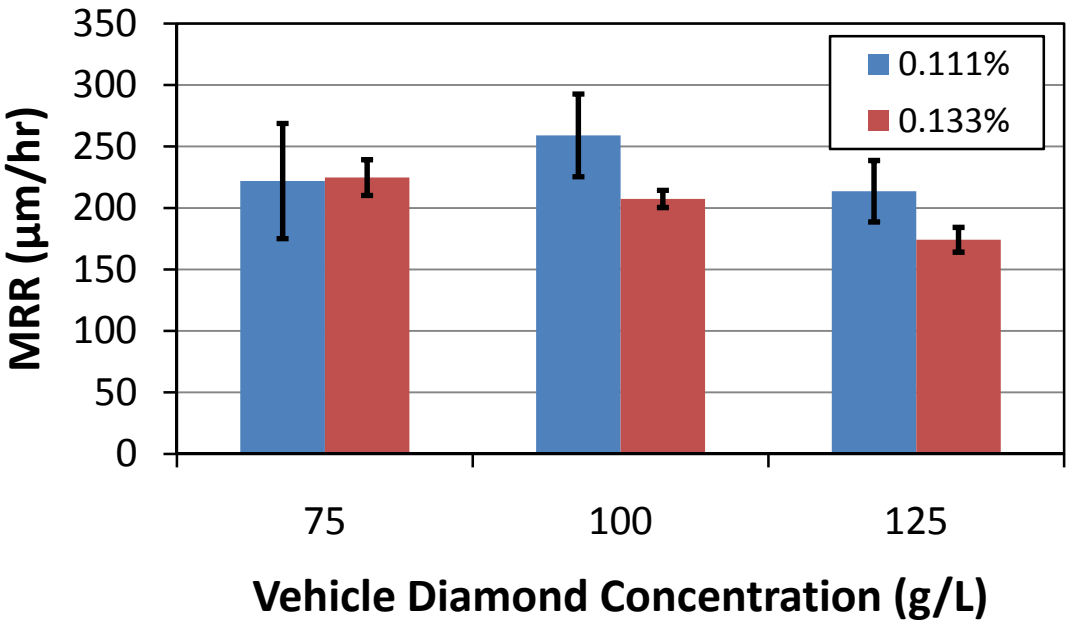

Figure 18. MRR results comparing vehicle concentrations with different abrasive values. Test parameters are in Table 10

Table 11. Tukey-Kramer HSD test p-values at 95% confidence level for results from Figure 18. Values not connected with bold p-values represents MRRs that are significantly different

Vehicle Carbomer Concentration (%), Vehicle Abrasive Concentration (g/L)	.111, 75	.111, 100	.111, 125	.133, 75	.133, 100	.133, 125
.111, 75	-	0.0009	***>0.9000***	***>0.9000***	***0.5852***	<0.0001
.111, 100	0.0009	-	<0.0001	0.0029	<0.0001	<0.0001
.111, 125	***>0.9000***	<0.0001	-	***0.8155***	***>0.9000***	0.0004
.133, 75	***>0.9000***	0.0029	***0.8155***	-	***0.3829***	<0.0001
.133, 100	***0.5852***	<0.0001	***>0.9000***	***0.3829***	-	0.0043
.133, 125	<0.0001	<0.0001	0.0004	<0.0001	0.0043	-

4.1.4. Water vs. Carbomer Lapping Fluid

A test was run using water as the lapping fluid instead of a carbomer based vehicle to determine its effect on MRR. The procedure for dispensing the diamonds and water to the lap plate are discussed in the Experimental Procedure section. The test parameters are shown in Table 12 and the results in Figure 19. The p-values from a Tukey-Kramer HSD test are listed in Table 13. These results show that using water as a lapping fluid produces significantly lower MRRs.

Table 12. Lapping parameters for results shown in Figure 19

Number of PDC Samples	18
Specimen Holder Material	Stainless Steel
PDC Layout Pattern	2-Ring
Abrasives	14/170 mesh mono-crystalline diamonds
Lap Plate Speed (RPM)	96
Pressure (KPa)	43.36
Vehicle Abrasive Concentration (g/L)	75
Vehicle Delivery Rate (L/min)	30

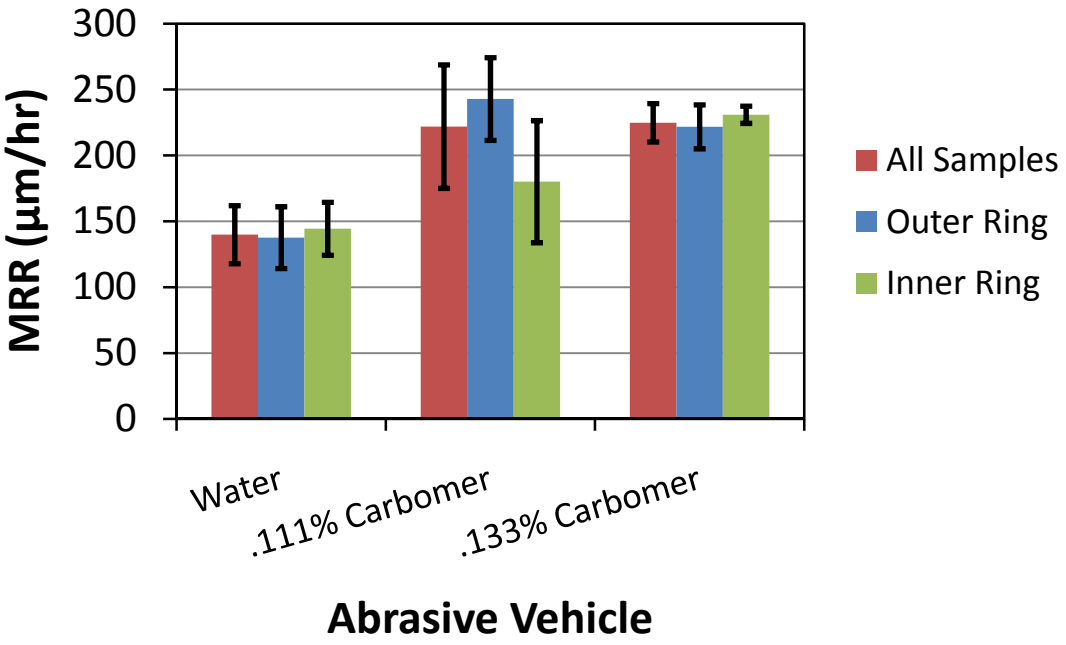

Figure 19. MRR results comparing the use of different abrasive vehicles. Refer to Table 12 for test parameters.

Table 13. Tukey-Kramer HSD test p-values at 95% confidence level for results from Figure 19. Sample holder values not connected with bold p-values represents MRR values that are significantly different.

Lapping Fluid	Water	0.111% Carbomer	0.133% Carbomer
Water	-	<0.0001	<0.001
0.111% Carbomer	<0.0001	-	***0.9591***
0.133% Carbomer	<0.0001	***0.9591***	-

4.1.5. Abrasive Grit Size Distribution

The diamond grit size distribution of purchased 140/170 mesh mono-crystalline diamond abrasives is shown in Figure 20. This distribution was obtained by sorting 1 kg

of abrasives with sieves. Two lapping tests were conducted using abrasives with more narrow grit size distributions than the 140/170 mesh diamonds. The results are shown in Figure 21 and the lapping parameters are shown in Table 14. Table 15 shows the p-values from a Tukey-Kramer HSD test. From the results it is shown that the 140/170 mesh abrasive grain size produces higher MRRs than both of the more narrow abrasive grain size distributions.

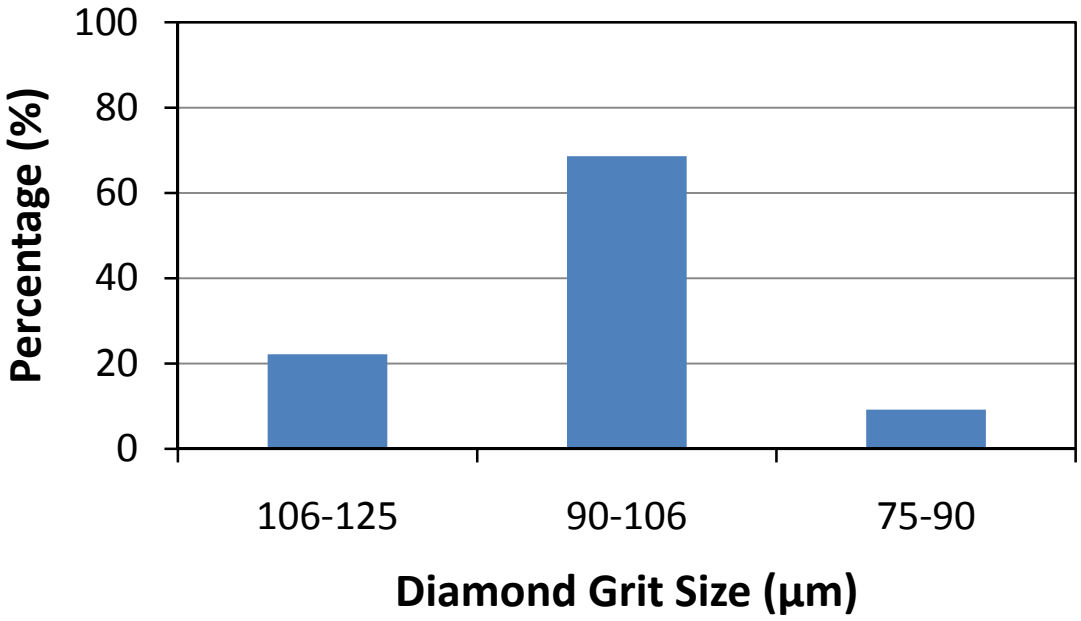

Figure 20. Size distribution of diamond grits from purchased 140/170 mesh polycrystalline diamond abrasives

Table 14. Lapping parameters for results shown in Figure 21

Number of PDC Samples	18
Specimen Holder Material	Stainless Steel
PDC Layout Pattern	2-Ring
Lap Plate Speed (RPM)	96
Pressure (KPa)	43.36
Vehicle Abrasive Concentration (g/L)	75
Vehicle Carbomer Concentration (%)	0.133
Vehicle Delivery Rate (L/min)	30

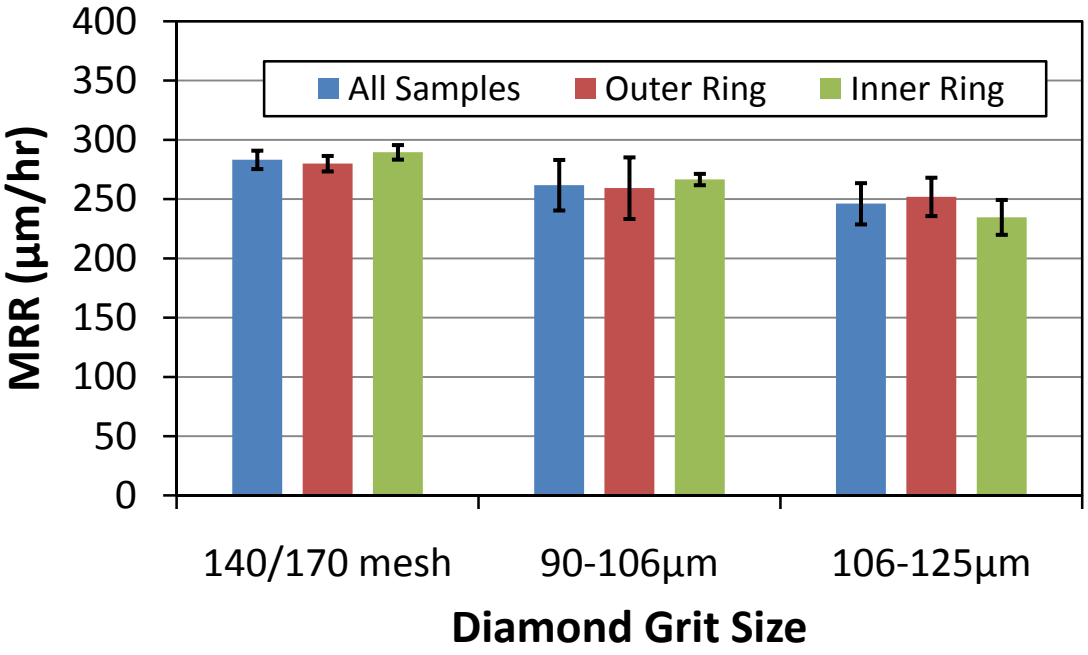

Figure 21. MRR results from lapping with specific diamond grit sizes.
Refer to Table 14 for test parameters.

Table 15. Tukey-Kramer HSD test p-values at 95% confidence level for results from Figure 21. Values not connected with bold p-values represent MRRs that are significantly different.

Diamond Distribution	140/170 mesh	90-106 microns	106-125 microns
140/170 mesh	-	0.0008	<0.0001
90-106 microns	0.0008	-	0.0179
106-125 microns	<0.0001	0.0179	-

4.1.6. Vehicle Abrasive Concentration and Pressure

Results comparing the MRR to various diamond concentrations at different pressures are shown in Figure 22. The lapping test parameters are in Table 16. Table 17 shows the p-values comparing the MRRs at the different test conditions. It is shown that the MRRs are not significantly different at the tested pressured when the vehicle diamond concentration is the same.

Table 16. Lapping parameters for results shown in Figure 22

Number of PDC Samples	18
Specimen Holder Material	Stainless Steel
PDC Layout Pattern	2-Ring
Abrasives	14/170 mesh mono-crystalline diamonds
Lap Plate Speed (RPM)	96
Vehicle Carbomer Concentration (%)	0.133
Vehicle Delivery Rate (L/min)	30

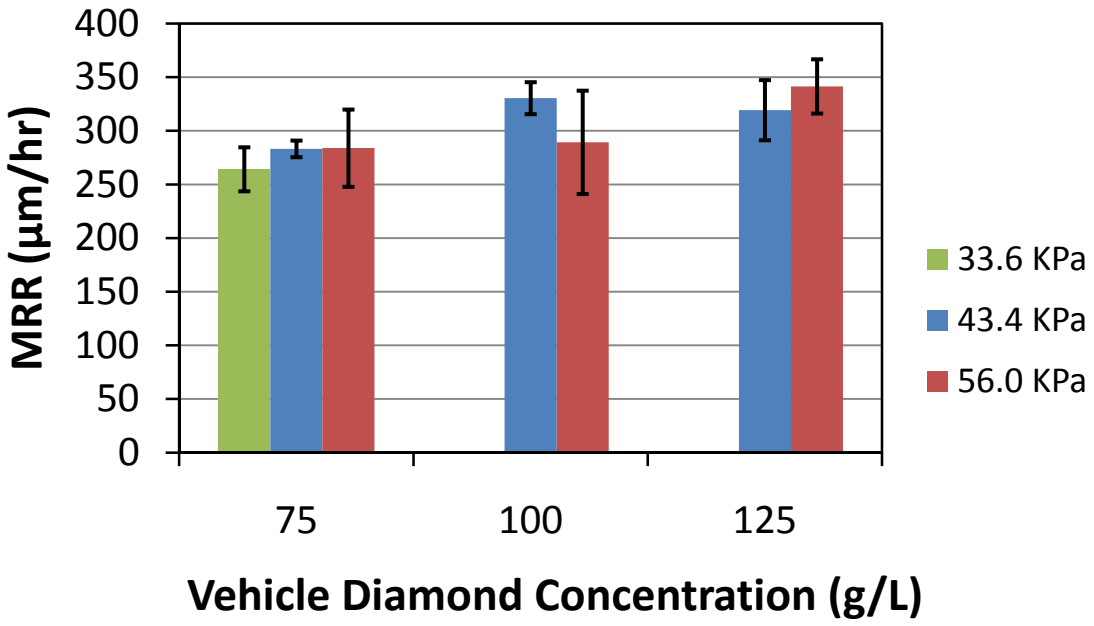

Figure 22. MRR results at various pressures and vehicle diamond concentrations. Refer to Table 16 for test parameters

Table 17. Tukey-Kramer HSD test p-values at 95% confidence level for results from Figure 22. Values not connected with bold p-values represents MRRs that are significantly different

Pressure (KPa), Abrasive Concentration (g/L)	33.6, 75	43.4, 75	56.0, 75	43.4, 100	56.0, 100	43.4, 125	56.0, 125
33.6, 75	-	***0.5825***	***0.5409***	<0.0001	***0.2465***	<0.0001	<0.0001
43.4, 75	***0.5825***	-	***>0.9000***	0.0006	***>0.9000***	0.0197	0.0015
56.0, 75	***0.5409***	***>0.9000***	-	0.0007	***>0.9000***	0.0238	0.0019
43.4, 100	<0.0001	0.0006	0.0007	-	**0.0044**	***>0.9000***	***>0.9000***
56.0, 100	***0.2465***	***>0.9000***	***>0.9000***	**0.0044**	-	***0.0923***	0.0103
43.4, 125	<0.0001	0.0197	0.0238	***>0.9000***	***0.0923***	-	***>0.9000***
56.0, 125	<0.0001	0.0015	0.0019	***>0.0009***	0.0103	***>0.9000***	-

4.1.6.1. Lap Plate Type

Pictures of the three different lap plate types tested are shown in Figure 23. Results comparing the MRR using different lap plate types are shown in Figure 24. The test parameters are in Table 18, and p-values comparing the MRRs at the different test conditions are in Table 19. The results show that there is no significant different between MRR and lap plate type.

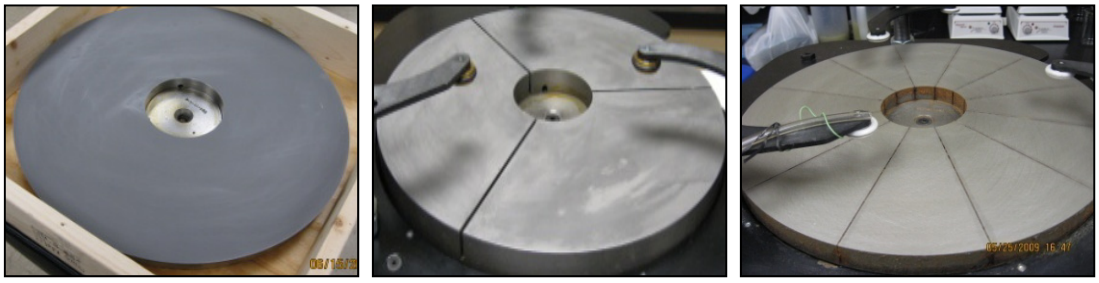

(a) (b) (c)

Figure 23. Lap plate types used. Cast iron: (a) solid (b) 3-slot (c) 12-slot

Table 18. Lapping parameters for results shown in Figure 24

Number of PDC Samples	18
Specimen Holder Material	Nitrile Rubber (57A)
PDC Layout Pattern	2-Ring
Abrasives	14/170 mesh mono-crystalline diamonds
Lap Plate Speed (RPM)	96
Pressure (KPa)	43.36
Vehicle Abrasive Concentration (%)	75
Vehicle Delivery Rate (L/min)	30

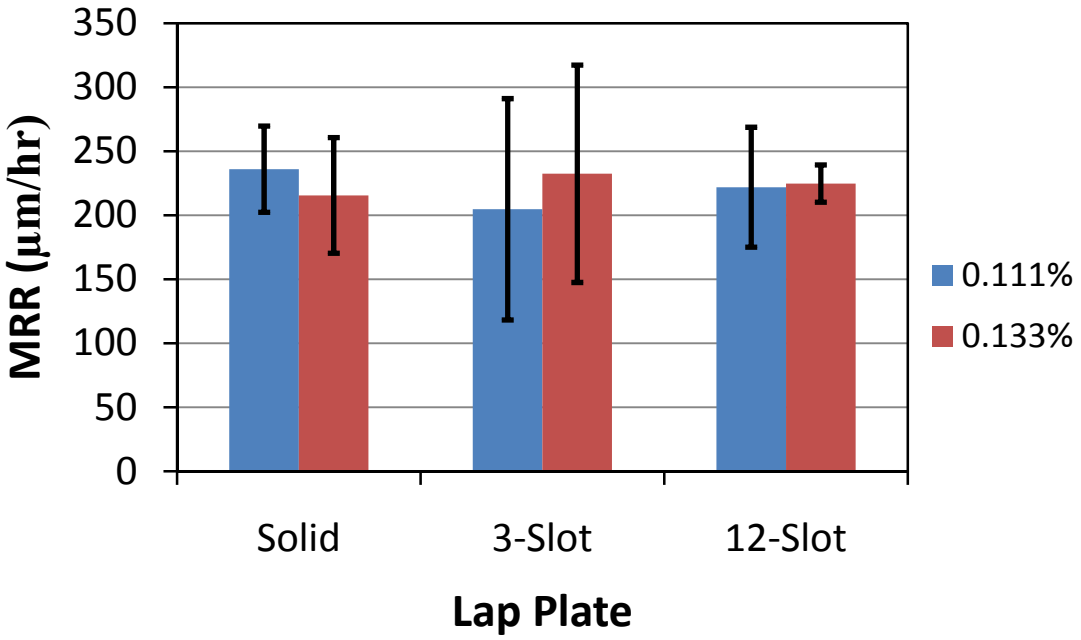

Figure 24. MRR results from different lap plate types. Refer to Table 18 for test parameters.

Table 19. Tukey-Kramer HSD test p-values at 95% confidence level for results from Figure 24. Values not connected with bold p-values represents MRRs that are significantly different.

Vehicle Carbomer Concentration (%), Lap Plate Type	0.111, solid	0.111, 3-slot	0.111, 12-slot	0.133, solid	0.133, 3-slot	0.133, 12-slot
0.111, solid	-	***0.8962***	***>0.9000***	***>0.9000***	***>0.9000***	***>0.9000***
0.111, 3-slot	***0.8962***	-	***0.5891***	***>0.9000***	***>0.9000***	***>0.9000***
0.111, 12-slot	***>0.9000***	***0.5891***	-	***0.7073***	***>0.9000***	***>0.9000***
0.133, solid	***>0.9000***	***>0.9000***	***0.7073***	-	***>0.9000***	***>0.9000***
0.133, 3-slot	***>0.9000***	***>0.9000***	***>0.9000***	***>0.9000***	-	***>0.9000***
0.133, 12-slot	***>0.9000***	***>0.9000***	***>0.9000***	***>0.9000***	***>0.9000***	-

4.1.6.2. Sample Holder Material

Several tests were conducted that compare the effects of using either a nitrile rubber or stainless steel sample holder. Figure 25 shows the MRR results of the two different sample holders at three different vehicle abrasive concentrations (75, 100, and 125 g/L), and the test parameters are shown in Table 20. It can be seen that at all vehicle abrasive concentrations the stainless steel sample holder produces a higher MRR. Table 21 shows the p-values that represent how the MRRs from the changing conditions relate to one another. It can be seen that the steel sample holder produces higher MRRs than the nitrile rubber sample holder at all diamond concentration values tested. Additionally, the steel sample holder produces higher MRRs when the vehicle abrasive concentration is either 100 or 125 g/L.

Additionally, several tests were conducted using nitrile rubber sample holders with different hardness values. Results from these tests compared to the use of a stainless steel sample holder are shown in Figure 26 and the parameters are in Table 22. The p-values that relate the tests MRRs to one another are shown in Table 23. These results show that the average MRR between the nitrile rubber sample holders does not vary significantly. The stainless steel sample holder however outperforms several more than half of the tested nitrile rubber sample holders. One possible reason for this is that the rubber holder allows the PDC more movement vertically, resulting in a less aggressive process.

Table 20. Lapping parameters for results shown in Figure 25

Number of PDC Samples	18
PDC Layout Pattern	2-Ring
Abrasives	14/170 mesh mono-crystalline diamonds
Lap Plate Speed (RPM)	96
Pressure (KPa)	43.36
Vehicle Carbomer Concentration (%)	0.133
Vehicle Delivery Rate (L/min)	30

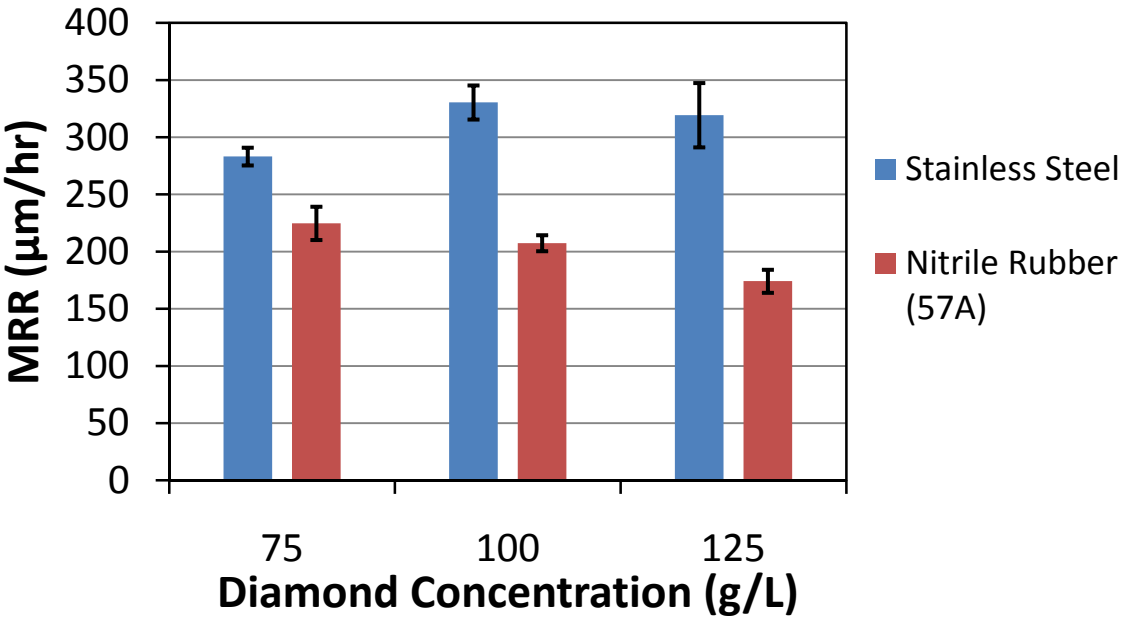

Figure 25. MRR results comparing a stainless steel and nitrile rubber specimen holder. Refer to Table 20 for test parameters

Table 21. Tukey-Kramer HSD test p-values at 95% confidence level for results from Figure 25. Values not connected with bold p-values represent MRRs that are significantly different.

Sample Holder Material, Vehicle Abrasive Concentration (g/L)	Steel, 75	Steel, 100	Steel, 125	Nitrile Rubber, 75	Nitrile Rubber, 100	Nitrile Rubber, 125
Steel, 75	-	<0.0001	<0.0001	<0.0001	<0.0001	<0.0001
Steel, 100	<0.0001	-	***0.2632***	<0.0001	<0.0001	<0.0001
Steel, 125	<0.0001	***0.2632***	-	<0.0001	<0.0001	<0.0001
Nitrile Rubber, 75	<0.0001	<0.0001	<0.0001	-	0.0132	<0.0001
Nitrile Rubber, 100	<0.0001	<0.0001	<0.0001	0.0132	-	<0.0001
Nitrile Rubber.125	<0.0001	<0.0001	<0.0001	<0.0001	<0.0001	-

Table 22. Lapping parameters for results shown in Figure 26.

Number of PDC Samples	18
PDC Layout Pattern	2-Ring
Abrasives	14/170 mesh mono-crystalline diamonds
Lap Plate Speed (RPM)	96
Pressure (KPa)	43.36
Vehicle Abrasive Concentration (g/L)	75
Vehicle Carbomer Concentration (%)	0.133
Vehicle Delivery Rate (L/min)	30

Table 23. Tukey-Kramer HSD test p-values at 95% confidence level for results from Figure 26. Sample holder values not connected with bold p-values represents MRR values that are significantly different.

Sample Holder	10A	20A	30A	40A	50A	60A	70A	80A	SS
10A	-	***0.1286***	***>.9000***	***0.8773***	***>.9000***	***0.5486***	***>.9000***	***0.2780***	***0.4124***
20A	***0.1286***	-	***0.2769***	***>.9000***	***0.8835***	***>.9000***	***0.4729***	***>.9000***	<.0001
30A	***>.9000***	***0.2769***	-	***>.9000***	***>.9000***	***0.7818***	***>.9000***	***0.4989***	***0.2148***
40A	***0.8773***	***>.9000***	***>.9000***	-	***>.9000***	***>.9000***	***>.9000***	***>.9000***	0.0107
50A	***>.9000***	***0.8835***	***>.9000***	***>.9000***	-	***>.9000***	***>.9000***	***>.9000***	0.0147
60A	***0.5486***	***>.9000***	***0.7818***	***>.9000***	***>.9000***	-	***>.9000***	***>.9000***	0.0015
70A	***>.9000***	***0.4729***	***>.9000***	***>.9000***	***>.9000***	***>.9000***	-	***0.7163***	***0.1029***
80A	***0.278***	***>.9000***	***0.4989***	***>.9000***	***>.9000***	***>.9000***	***0.7163***	-	0.0003
SS	***0.4124***	<.0001	***0.2148***	0.0107	0.0147	0.0015	***0.1029***	0.0003	-

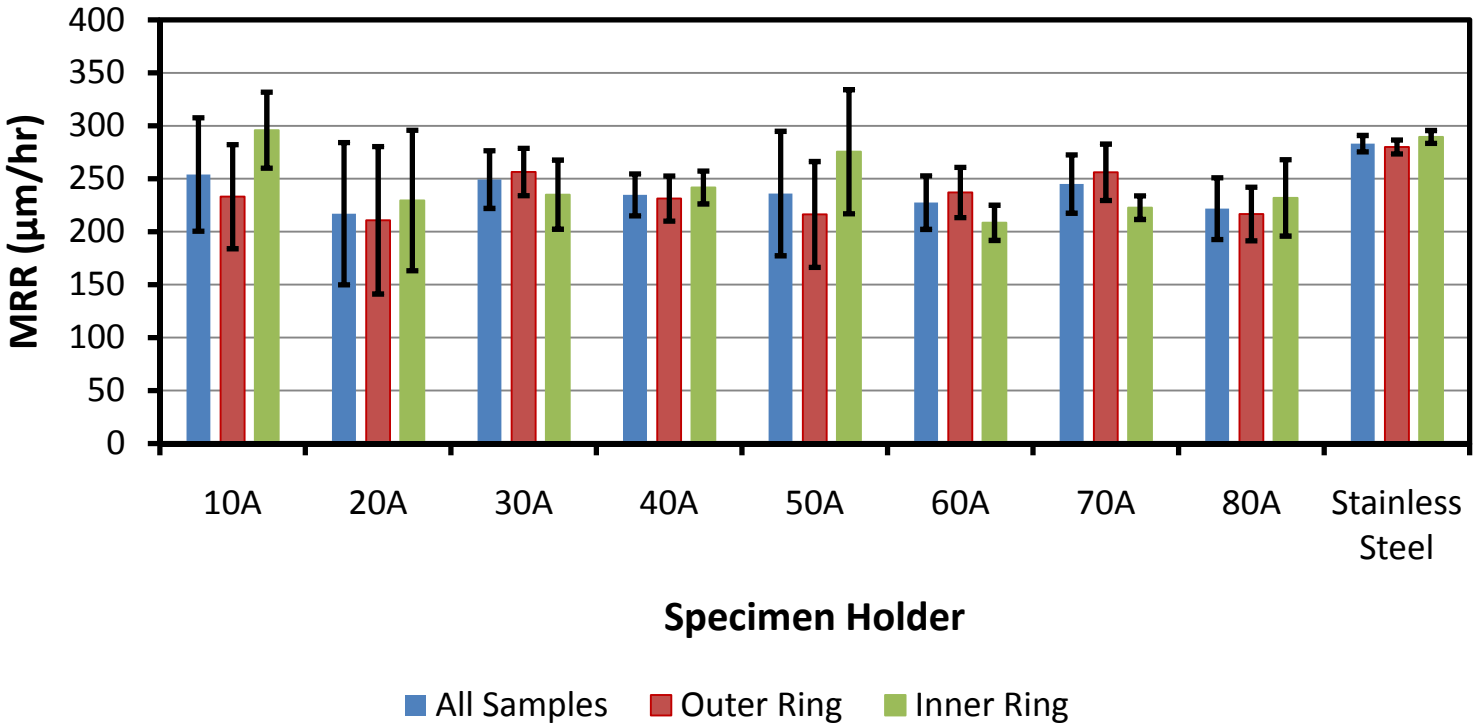

Figure 26. MRR based on nitrile rubber specimen holder hardness values (Shore A scale) and stainless steel holder

4.1.6.3. PDC Density and Layout

Five different PDC sample holder designs were tested to determine how well they would perform. The layouts are shown in Figure 27. The sample holder shown in Figure 27d has 28 samples on the outer ring and 14 on the inner ring. The constant test parameters are listed in Table 24. The vehicle flow rate was changed between sample holder designs to a flow rate of 1.667 mL/min per PDC sample on the holder. This flow rate results in the standard flow rate of 30 mL/min per 18 samples which was commonly used in previous tests. Note that the weight applied to the samples was also increased with increases in PDCs to achieve the same pressure. The results from the different tests are shown in Figure 28. Overall, the 28 sample layout has the highest average MRR. Table 25 shows the p-values from a Tukey-Kramer HSD test that compares the MRRs between the sample holder layouts. From the results it can be seen that the only sample holders that have significantly different MRRs from one another are 18 sample, 1-ring layout and the 28 sample, 1 ring layout.

Additionally, two more tests were performed using the 28 sample, 1-ring layout pattern. The results from these tests and the test conditions are shown in Figure 29 and Table 26, respectively. P-values from a Tukey-Kramer HSD test are listed in Table 27, and the results show that while using the same abrasive consumption rate with a different amount of lapping fluid, there is no significant difference in the MRR.

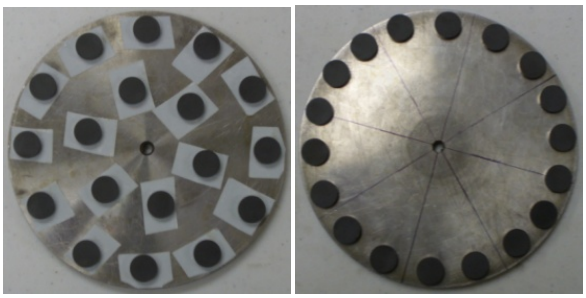

(a) (b)

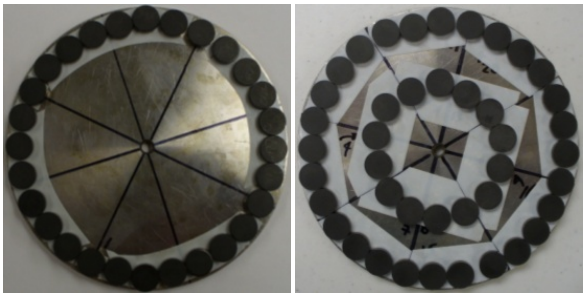

(c) (d)

Figure 27. Pictures of specimen holders and layouts. Stainless Steel –
(a) 18 samples / 2-ring, (b) 18 samples / 1-ring, (c) 28 samples / 1-ring,
(d) 42 samples / 2-ring

Table 24. Test parameters for results listed in Figure 28

Specimen Holder Material	Stainless Steel
Abrasives	14/170 mesh mono-crystalline diamonds
Lap Plate Speed (RPM)	96
Pressure (KPa)	43.36
Vehicle Abrasive Concentration (g/L)	75
Vehicle Carbomer Concentration (%)	0.133

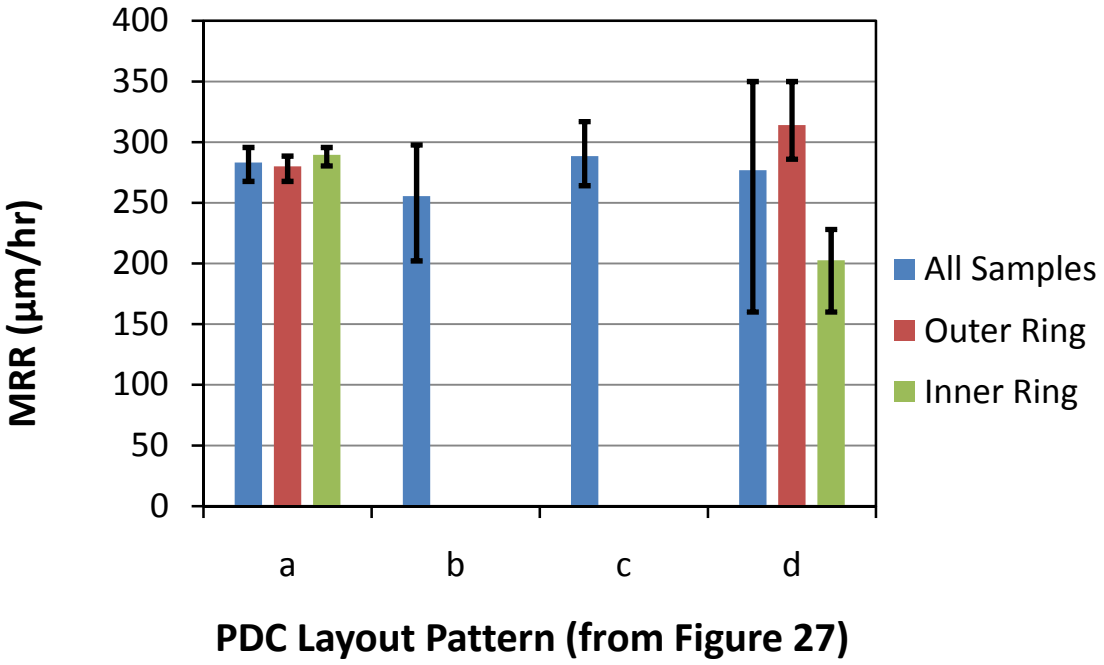

Figure 28. MRR results from specimen holder layout tests. Refer to Figure 27 for layout patter designs and Table 24 for test parameters

Table 25. Tukey-Kramer HSD test p-values at 95% confidence level for results from Figure 28. Sample holders not connected by a bold p-value represent MRRs that are significantly different

Sample Holder	(b) 18: 1 Ring	(a) 18: 2-ring	(c) 8: 1-ring	(d) 42: 2-ring
(b) 18: 1 Ring	-	***0.1219***	0.0213	***0.1787***
(a) 18: 2-ring	***0.1219***	-	***0.9651***	***0.9334***
(c) 8: 1-ring	0.0213	***0.9651***	-	***0.5834***
(d) 42: 2-ring	***0.1787***	***0.9334***	***0.5834***	-

Table 26. Test parameters from results in Figure 29

Number of PDC Samples	28
PDC Layout Pattern	1-ring
Specimen Holder Material	Stainless Steel
Abrasives	14/170 mesh mono-crystalline diamonds
Lap Plate Speed (RPM)	96
Pressure (KPa)	43.36

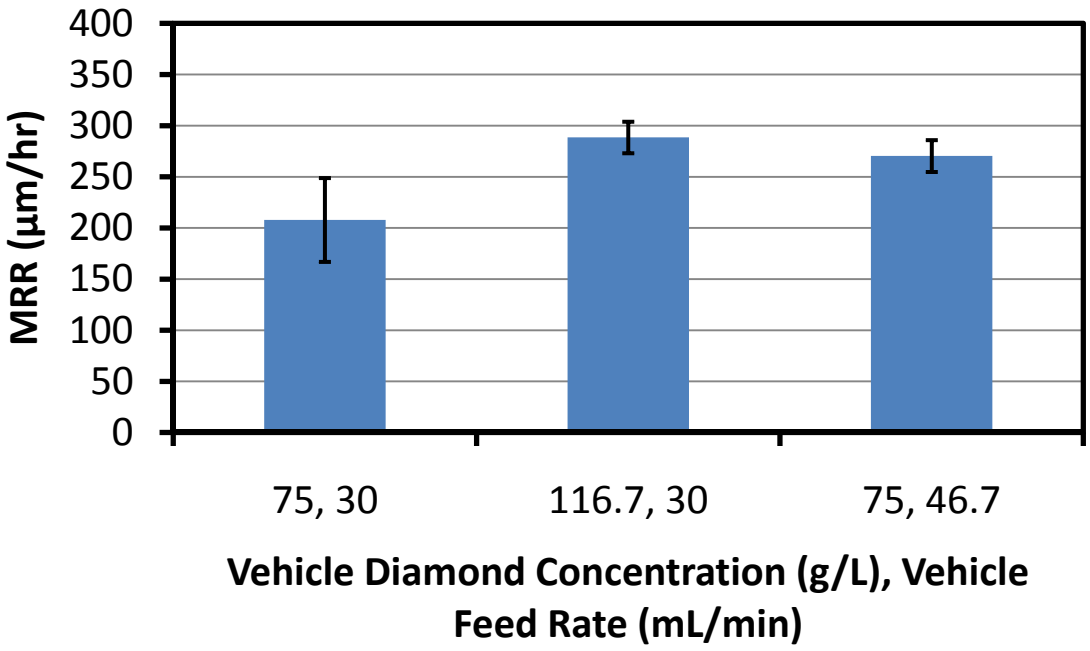

Figure 29. MRR results from the 28 sample, 2-ring PDC layout design.
Refer to Table 26 for test parameters

Table 27. Tukey-Kramer HSD test p-values at 95% confidence level for results from Figure 29. Values not connected by a bold p-value represent MRRs that are significantly different

Vehicle Flow Rate (mL/min), Vehicle Diamond Concentration (g/L)	30, 75	30, 116.67	46.67, 75
30, 75	-	<0.0001	<0.0001
30, 116.67	<0.0001	-	0.0146
46.67, 75	<0.0001	0.0146	-

4.2. Surface Analysis

The surface roughness of the PDCs was measured after several lapping tests at various pressures and lap plate speeds, and the results are shown in Figure 30. Note that all other variables were held constant as shown in Table 5. A Tukey-Kramer HSD test was performed on the results to compare the different tests and the results are in Table 28. It is shown that as the pressure and velocity increase, the average surface roughness, Ra, decreases. Roughness measurements were also collected from the PDCs that were lapped in the 42 sample, 2-ring design. The results are listed in Table 29. A Student's t-test was used to compare the roughness values, and it was found at a 95% confidence level that the average roughness of the inner and outer samples were different based on a p-value of less than 0.0001.

Scanning Electron Microscope images were taken of the surface of PDCs after lapping and are shown in Figure 31. Figure 31a and b show two locations where the surface has clearly been affected by brittle material fracture with no presence of ductile

material removal. Figure 31c and d are lower magnifications of the surface that illistrate the PDC surface topography.

Figure 32 and Figure 33 show digital microscope pictures of pits in the PDC surface after lapping at a pressure of 56 KPa.

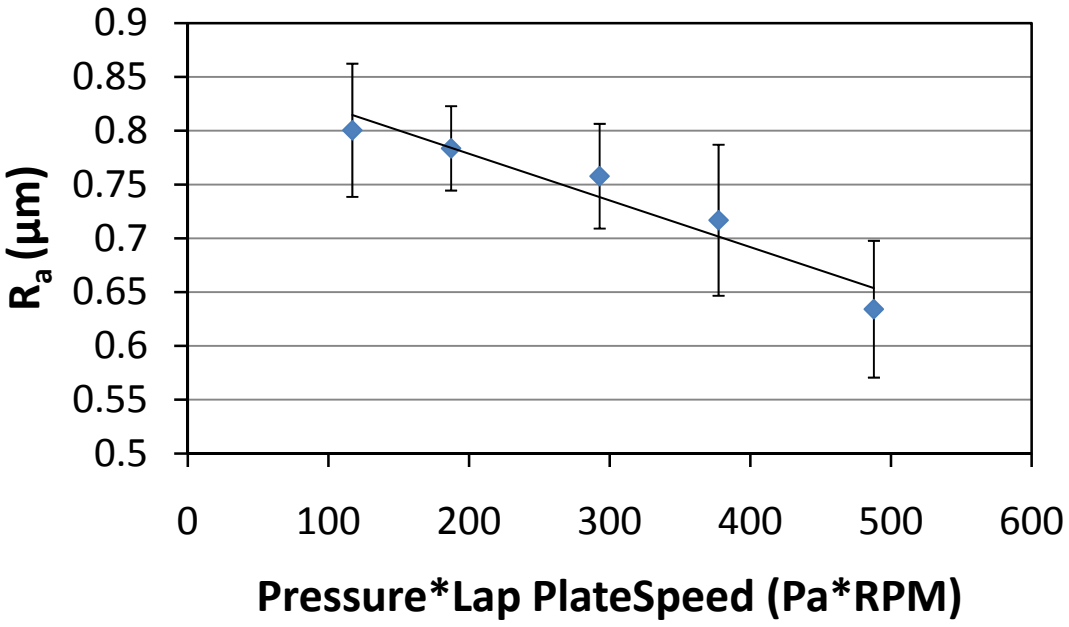

Figure 30. Surface roughness results as a function of pressure and lap plat speed

Table 28. Tukey-Kramer HSD test p-values at 95% confidence level for results from Figure 30. Pressure-velocity values not connected with bold p-values represent roughness values that are significantly different

Pressure * Velocity (KPa*m/s)	117	187.2	292.8	377.4	487.8
117	-	***0.9241***	***0.2463***	***0.0015***	<.0001
187.2	***0.9241***	-	***0.7170***	0.0170	<.0001
292.8	***0.2463***	***0.7170***	-	***0.2867***	<.0001
377.4	***0.0015***	0.0170	***0.2867***	-	0.0018
487.8	<.0001	<.0001	<.0001	0.0018	-

Table 29. Average roughness measurements and standard deviations from lapping 42 samples in a two-ring layout pattern

Ra (µm)	Inner Ring	Outer Ring
	0.566 ± 0.099	0.695 ± 0.111

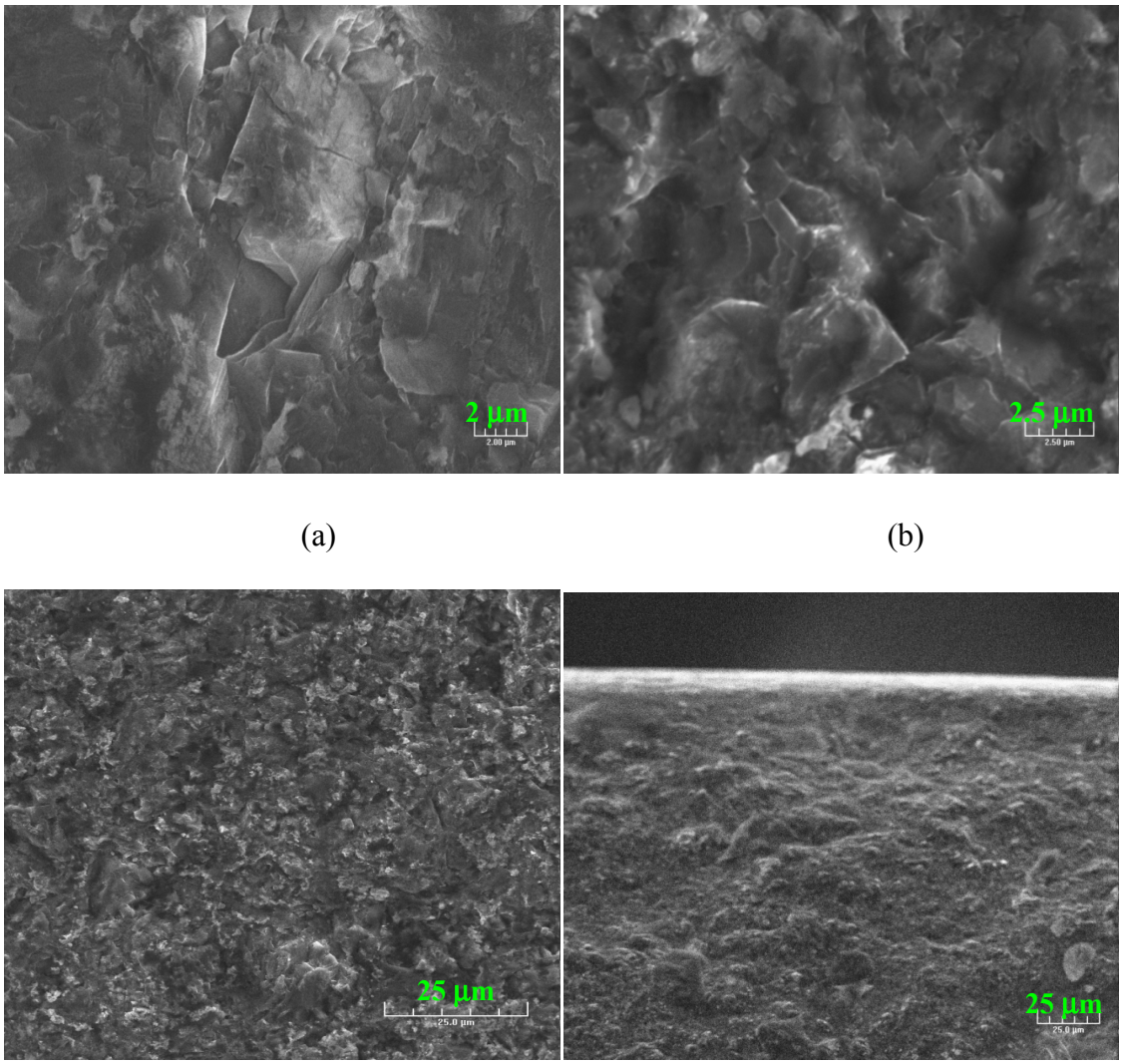

Figure 31. SEM images of the PDC surface post lapping at (a &b) 6000X (c) 1000X (d) 500X

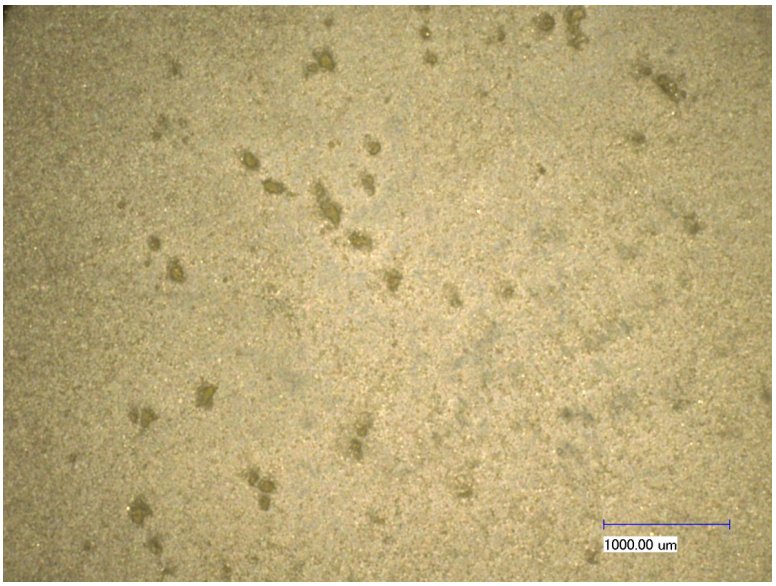

Figure 32. Image of the pits on the surface of a PDC after lapping at 56 KPa (50X)

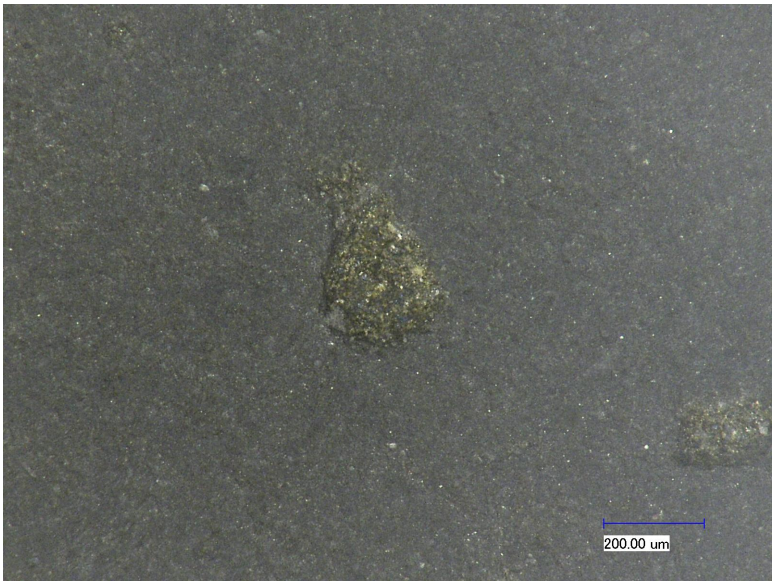

Figure 33. Image of the pits on the surface of a PDC after lapping at 56 KPa (200X)

4.3. Reclaimed Diamond Analysis

The collected sludge after lapping at several different pressures was collected and sorted into groups according to size. Figure 34 shows the results, and it can be seen that there are a greater number of diamond with larger grit sizes when lapped at lower pressures. Digital microscope images of purchased mono-crystalline diamond abrasives are shown in Figure 35, and Figure 36 shows SEM images of reclaimed diamond abrasives. Comparing the images shows that the "bulky" shape of the abrasives is retained after being crushed during lapping.

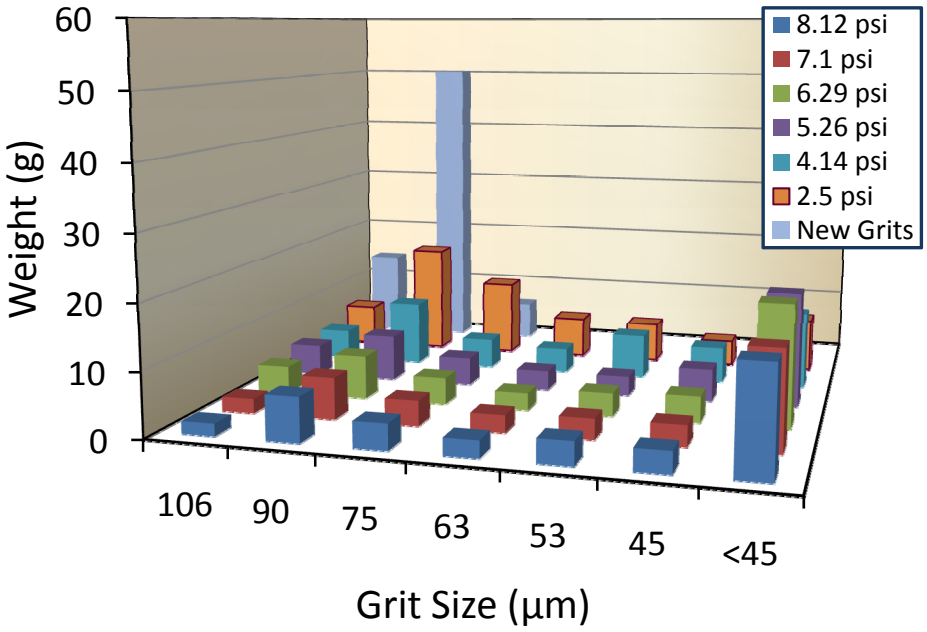

Figure 34. Analysis of reclaimed diamond grit size after lapping at different pressures

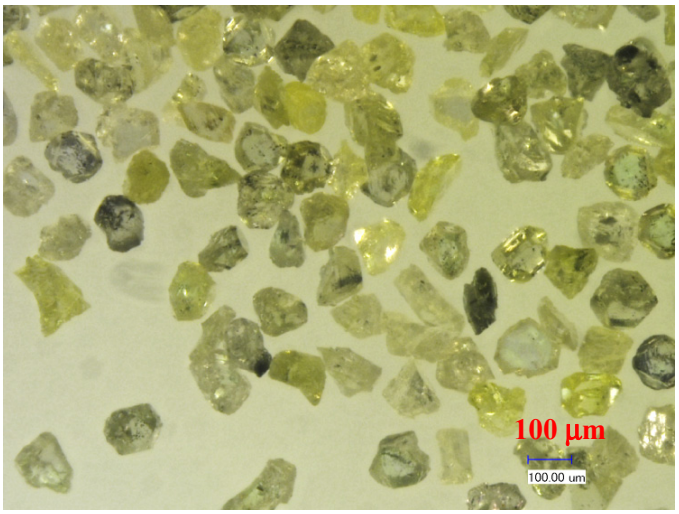

(a)

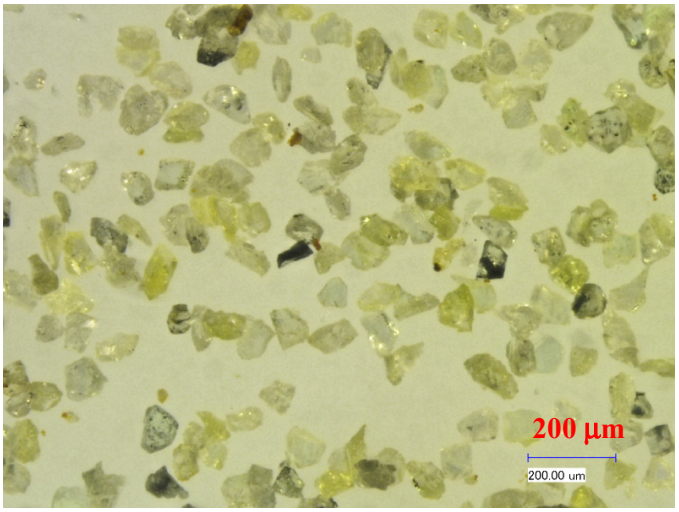

(b)

Figure 35. Purchased mono-crystalline diamond abrasives of grit size ranges: (a) 90-106 µm (b) 46-53 µm

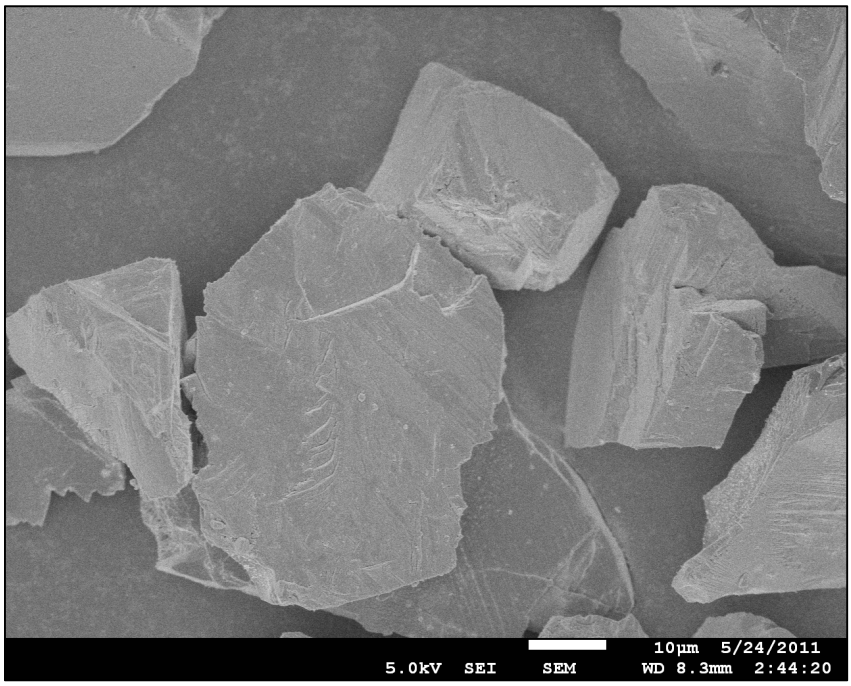

(a)

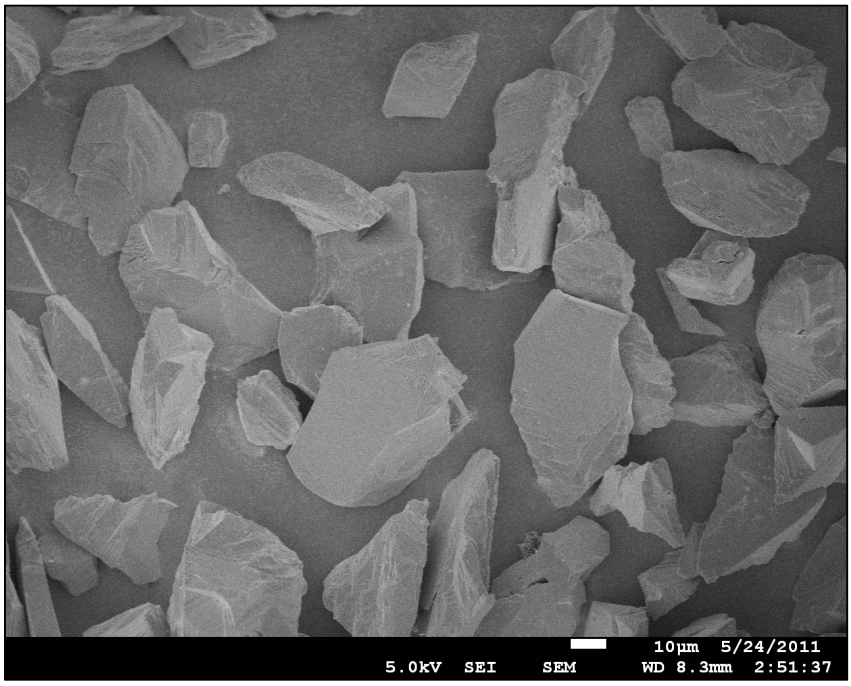

(b)

Figure 36. (a-b) SEM images of reclaimed diamond after lapping

CHAPTER V

MECHANISMS OF MATERIAL REMOVAL AND PROCESS OPTIMIZATION

This chapter discusses the mechanisms of material removal and process optimization from the results in Chapter IV. The different lapping parameters that were tested will be discussed in relation to how they affect the lapping of PDCs. Additionally, the MRR uniformity will be discussed.

5.1. Pressure, Velocity, and Abrasive Consumption Rate

From the results shown in Figure 13 and Figure 14, the MRRs can be plotted against the applied pressure and average velocity of the PDC samples. The average velocity of the samples located on the inner and outer ring of the sample holder is calculated with Equation 3. Figure 37 shows the results from the tests which used a stainless steel sample holder and results from data previously obtained using a nitrile rubber sample holder. From the graph it is seen that the MRR increases linearly with increases in pressure or speed as Preston's equation, Equation 1, predicts. The MRR however does not increase after reaching a critical pressure and velocity which agrees with previous research on the modeling of Preston's equation [19, 26, 27, 29, 37-39]. Also shown in Figure 37 is that by using a stainless steel instead of a nitrile rubber sample holder, higher MRRs can be achieved. This finding agrees with the results shown in Figure 25. The results also show that MRRs in excess of 280 μm/hr can be achieved which is a substantial improvement from what is seen in industry.

Another finding can be seen when looking at the results presented in Figure 13 and Figure 14. Table 30 shows p-values from a Student's t-test that compares the MRR

of the inner and outer samples on the sample holder at different pressures and speeds. The smallest p-values, which represent the tests that had the largest difference in MRR between the inner and outer samples, occurs at a pressure of 56.05 KPa. This result along with the observation that pits form in samples lapped at this highest tested pressure, as shown in Figure 32, lead to the conclusion that the lapping pressure should not be increased above around 45 KPa. This is not an issue when modeling the test procedures in this research and lapping at 96 RPM because the maximum MRR is achieved at a lower pressure. However, it would need to be taken into account when lapping at slower speeds and trying to achieve higher MRRs by increasing the applied pressure.

Table 30. P-values from Student's t-test at a 95% confidence interval comparing the average MRRs between the inner ring and outer ring samples. Note that p-values in bold represent samples that have a significantly different MRR.

Pressure (KPa)	p-value	
	60 RPM	96 RPM
13.44	0.6826	***0.0078***
33.64	0.2538	0.9433
43.36	0.7790	0.2882
56.05	***0.0042***	***<0.0001***

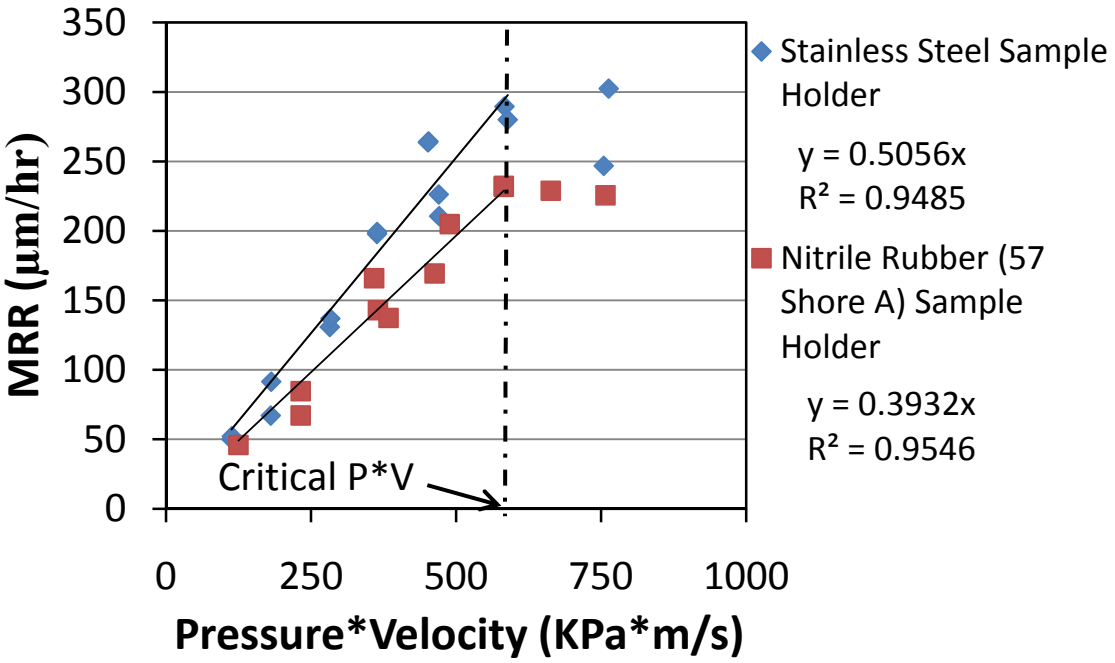

Figure 37. PDC MRR based on applied pressure and average sample velocity

Based on the results in Figure 16 and Figure 17 which varied the vehicle abrasive concentration and vehicle feed rate, respectively, the MRR can be plotted against the abrasive consumption rate as shown in Figure 38. Note that this consumption rate is based on sample holder with 18 PDC samples. A Student's t-test comparison at a 95% confidence interval was performed, and at a diamond consumption rate of 0.75 g/min there is a difference between the MRR based on the amount of supplied lapping fluid (p-value < 0.0003). At higher diamond consumption rates there is no difference between the amount of supplied lapping fluid and the MRR (p-values > 0.0001). This finding agrees with the results presented in Figure 29 for the sample holder with 28 samples in a 1-ring

design pattern. It is also shown that a maximum MRR in excess of 300 µm/hr can be achieved when lapping with an abrasive consumption rate of around 3 g/min.

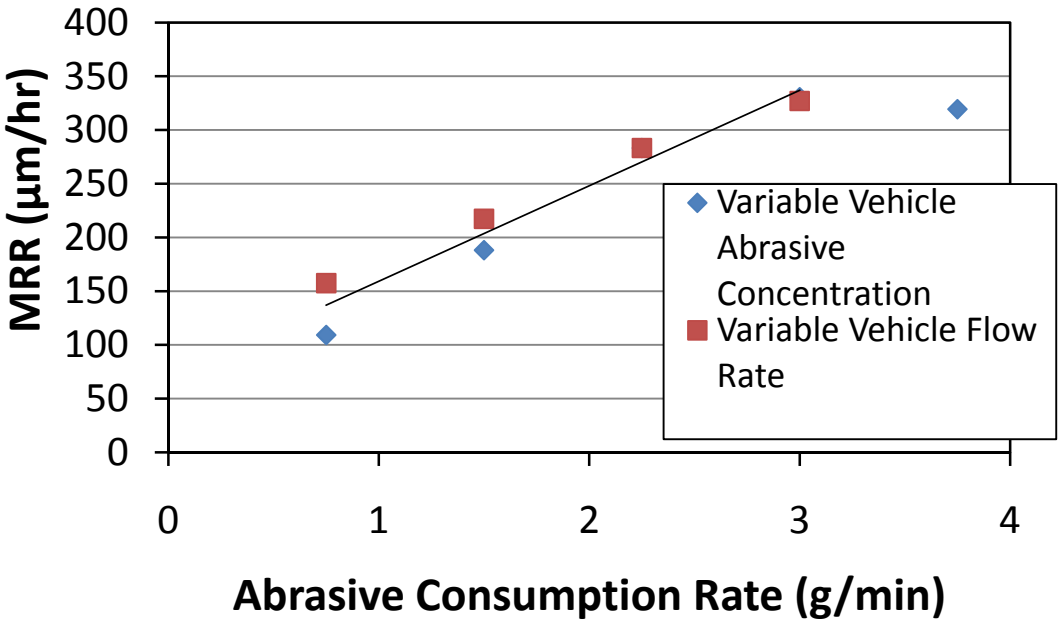

Figure 38. MRR based on abrasive consumption rate

The average surface roughness measurements that were presented in Figure 30 are all below 1 µm which meet the typical surface finish requirement. However, these surface finishes would be improved even more during the finishing stage of the lapping process when smaller grit size abrasives are used. The decrease in surface roughness as pressure and velocity increase is likely due to the aggressiveness of the wear process. That is, at higher velocities and pressures the abrasives are crushed into smaller pieces.

There are therefore a greater number of active smaller grit abrasives, and this results in better surface finishes because of the smaller abrasive size as shown from previous work [35, 45-47].

5.2. Lapping Vehicle

The use of a carbomer based lapping vehicle was decided on based the standard used in industry. This type of suspension vehicle works well for the lapping process because of its shear-thinning property which can be seen in Figure 39. The viscosity of the fluid aids in suspending the abrasives moving the abrasives along the lap plate. The shear stress exhibited on the fluid as it moves between the lap plate and conditioning ring or workpiece reduces the viscosity of the fluid which allows it to run off the lap plate. Previous research conducted with non-shear-thinning suspension vehicles has resulted in problems due to the buildup of lapping fluid on the lap plate. The results shown in Figure 18 compare MRRs from tests from carbomer based vehicles with different viscosities. At vehicle abrasive concentrations of 100 and 125 g/L, the 0.111% carbomer vehicle, or lower viscosity vehicle, produces higher MRRs which does not agree with previous reports on the effect viscosity has on MRR [41]. However, Figure 19 which compares the use of water as a lapping vehicle to the carbomer vehicle, shows that using water for an abrasive vehicle will significantly reduce the process MRR.

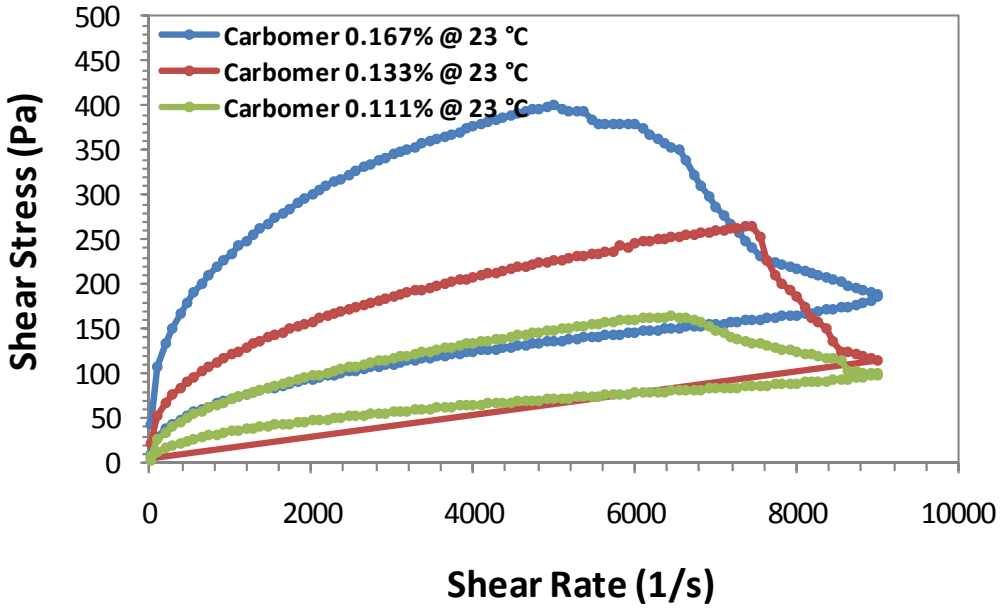

Figure 39. Shear stress vs. shear rate of carbomer based lapping vehicle

5.3. Abrasive Distribution and Lap Plate Type

Results that were reported in Figure 21 show that the larger abrasive grit size distribution (106-125 µm), had a significantly lower MRR than the 90 to 106 µm abrasive grit size. This is interesting because based on previous work, it would be expected that larger abrasives would result in higher MRRs [36, 43]. However, this is not an issue specific to this process because the standard size abrasives, 140/170 mesh, for this process had a higher MRR than the more narrow grit size distributions.

Another parameter that was shown to have no effect on the MRR was the lap plate type (Figure 24). The slotted style lap plates were studied because of research that

showed the MRR would increase if the lapping process design supported the removal of used abrasives and vehicle [39].

5.4. Sample Holder Material

The use of a nitrile rubber sample holder was chosen based on a recommendation from a company that manufactures lapping machines and products. The stainless steel sample holder was chosen because most companies that lap PDCs have a carrier that is made from stainless steel.

The results in Figure 25 show that higher MRR can be achieved when using a stainless steel sample holder. Additionally, the MRR variation between samples lapped with stainless steel sample holders is less than when lapped with nitrile rubber sample holders. It is believed that the greater variation can be attributed to the hardness of the material. Figure 40 shows quantile and density plots of PDCs that were lapped on nitrile rubber and stainless steel sample holders. It can be seen that the MRR is more normal among the samples lapped on the stainless steel sample holder.

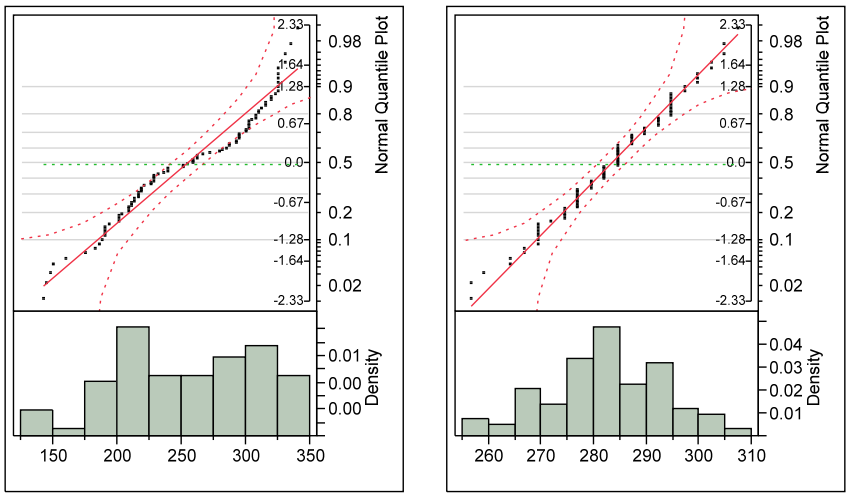

(a) (b)

Figure 40. Quantile and density plots from tests run with sample holders made from (a) 10A nitrile rubber (b) stainless steel

5.5. PDC Layout Design

The 18 sample, 2-ring PDC layout pattern that was used for the majority of this research was based on designs that are seen in industry. That is, the PDCs are placed in concentric circles on the sample holder and are separated from one another. The 28 sample, 1-ring and 42 sample, 2-ring designs were used to see if the process productivity could be increased by increasing the PDC density on the sample holder.

It is important to note that the same diamond consumption rate per PDC sample is being used in the results presented in Figure 28. That is, all test are using 7.5 g/hr per PDC being lapped. In comparing the sample holders that only have 18 samples, there is not a significant difference between the MRRs. Productivity can obviously be increased

by increasing the number of samples on the sample holder in using the 28 sample, 1-ring design, because it also has the same MRR.

In comparing the 28 sample design the 42 sample design, both have the same average MRRs among samples. However, the problem with the 42 sample design is that when comparing the MRR of the samples on the inner and outer ring, there is a significant difference between the MRR (p-value < 0.0001). It is believed that this is due to the abrasives being crushed to smaller sizes before reaching the inner samples. This is not a problem in the 18 sample, 2-ring design, because there is space between the samples which allows the diamonds to pass. One possible solution to working around this problem would be to distribute abrasive vehicle to the center of the sample holder during lapping. The inner samples on the 42 ring design also have a better surface finish as shown in Table 29, which supports the conclusion that smaller abrasive particles are engaged with the inside samples.

5.6. Material Removal Rate Uniformity

As discussed previously, it was found that using a stainless steel sample holder produced more uniform MRRs among samples lapped on the same sample holder. Throughout this research the MRR deviation between samples lapped on the same sample holder using the stainless steel holder was constantly below 25 μm. Due to the limited number of samples available for this research, a more in depth statistical analysis on whether there are correlations between other process parameters and to what extent they affect the uniformity was not possible. It is likely that the original variation between the samples thicknesses plays a role in uniformity. It is also conceivable that the

uniformity cannot be improved from what was obtained with the lapping conditions that were used for this research. If the finishing stage of the lapping process were to be examined, the results from this study could be used to determine how abrasive size affects MRR uniformity. Based on research that has been conducted[47], it is likely that an increase in MRR uniformity would be seen due to the smaller abrasive size.

CHAPTER VI

CONCLUSIONS AND FUTURE WORK

6.1. Conclusions

This investigation studied the lapping process of PDCs and how the lapping parameters chosen affect the MRR during the roughing stage of the process. The pressure, velocity, abrasives, vehicle, sample holder, lap plate, and sample layout were all investigated. Findings from this experiment can be used to improve the current process seen in industry and the summarized conclusions are:

1. MRRs in excess of 300 μm/hr can be achieved. In this research this was accomplished at a lap plate speed of 96 RPM on a 15" lap plate at a pressure of 43.46 KPa. The diamond abrasive consumption rate was 10 g/hr per PDC sample, and a carbomer based suspension vehicle was used.
2. The lapping productivity can be optimized from current PDC layout patterns that use a series of concentric circles with PDCs placed separated from one another. It was shown that PDCs placed in one concentric circle touching one another will achieve the same MRRs.
3. Stainless steel sample holders will achieve higher MRRs than sample holders made from rubber materials. There is no difference in the MRR when using solid lap plates in comparison to lap plates with slotted partitions.
4. The MRR uniformity of lapped PDC samples is increased when lapping with stainless steel instead of nitrile rubber sample holders. MRR deviations of less than 25 μm were consistently obtained.

5. The MRR when lapping PDCs can be accurately modeled by the Preston equation below a critical pressure and velocity level.

The importance of this research is in developing a greater understanding of how different parameters affect the lapping process specifically to the manufacturing of PDCs. The lapping process for PDCs can now be improved by adjusting the controllable process variables. It has been shown that MRRs of more than two times what is currently seen in industry can be achieved.

6.2. Future Work

The roughing stage during the lapping process for manufacturing PDCs has been studied. The effects of several controllable parameters on the MRR have been shown. There are several areas of research that can still be studied to improve the understanding and process that include:

1. The results presented can be verified through a series of more tests. The test results can also be used to determine if there are correlations between the variable lapping parameters and the MRR uniformity of samples lapped together.
2. The processes can be transitioned to and studied on larger lapping machines.
3. The finishing stage of the manufacturing process can be studied.

REFERENCES

1. Zhang, G.E., "An Experimental Study on Laser Cutting Mechanisms of Polvcrvstalline Diamond Compacts." *CIRP annals*, Vol. 56, 2007, pp. 201-204.
2. Catledge, S.A., "Micro-raman Stress Investigations and X-ray Diffraction Analysis of Poly Crystalline Diamond (PCD) Tools." *Diamond and Related Materials*, Vol. 5(10), 1996, pp. 1159-1165.
3. Jia, H., "Research On Polycrystalline Diamond Compact (PDC) with Low Residual Stress Prepared Using Nickel-based Additive." *International Journal of Refractory Metals and Hard Materials*, Vol. 29, 2011, pp. 64-67.
4. Miess, D., "Fracture Toughness and Thermal Resistance of Polycrystalline Diamond Compacts." *Materials Science & Engineering: Structural Materials, Properties, Microstructure and Processing*, Vol. 1-2, 1996, pp. 270-276.
5. Ohno, T., "Cost Reduction of Polycrystalline Diamond Compact Bits Through Improved Durability." *Geothermics*, Vol. 31(2), 2002, pp. 245-262.
6. Singh, B., "Study of Polycrystalline Sintered Compacts of Diamond." *Journal of Materials Science*, Vol. 22(7), pp. 2407-2410.
7. Fang, A., "Lapping of Polycrystalline Diamond Compact (PDC)." *Advanced Materials Research*, Vol. 126-128, 2010, pp. 469-474.
8. Bogdanov, G., "Non-destructive Testing of Polycrystalline Diamond Cutters Using DC Electrical Conductivity Imaging." *Measurement Science & Technology*, Vol. 20(9), 2009.

9. Lin, T. P., "Residual Stresses in Polycrystalline Diamond Compacts." *Journal of the American Ceramic Society*, Vol. 77(6), 1994, pp. 1562-1568.

10. Hamade, R.F., "Compact Core Drilling in Basalt Rock Using PCD Tool Inserts: Wear Characteristics and Cutting Forces." *Journal of Materials Processing Technology*, Vol. 210(10), 2010, pp. 1326-1339.

11. Hibbs Jr, L.E. and Lee, M., "Some Aspects of the Wear of Polycrystalline Diamond Tools in Rock Removal Processes." *Wear*, Vol. 46, 1978, pp. 141-147.

12. Ersoy, A., "Drilling Detritus and the Operating Parameters of Thermally Stable PDC Core Bits." *International Journal of Rock Mechanics and Mining Sciences*, Vol. 34(7), 1997, pp. 1109-1123.

13. Guo-Ping, X., "Micro-Raman Stress Investigation of Polycrystalline Diamond Compact (PDC)." *Advanced Materials Research*, Vol. 76-78, 2009, pp. 690-695.

14. Krawitz, A.D., "Residual Stresses in Polycrystalline Diamond Compacts." *International Journal of Refractory Metals and Hard Materials*, Vol. 17, 1999, pp. 117-122.

15. Zhang, Y., "High Pressure and High Temperature Sintering of Fine-grained PCD Using Bi-layered Assembly." *High Pressure Research*, Vol. 29(2), 2009, pp. 325-334.

16. Marinesscu, I., Uhlmann, E., and Doi, T., "*Handbook of Lapping and Polishing*," Taylor & Francis Group, Boca Raton, FL, 2007.

17. Fang, L., "Movement Patterns of Abrasive Particles in Three-body Abrasion." *Wear*, Vol. 162-164(2), 1993, pp. 782-789.

18. Dwyer Joyce, R.S., "Investigation into the Mechanisms of Closed Three-body Abrasive Wear." *Wear*, Vol. 175, 1994, pp. 133-142.

19. Tseng, W. T., "Re-examination of Pressure and Speed Dependences of Removal Rate During Chemical-mechanical Polishing Processes." *Journal of the Electrochemical Society*, Vol. 144(2), 1997, pp. L15-L17.

20. Lin, T. R., "Optimization of Removal Rate and Weibull Modulus in Polishing of Ceramic Blocks Using the Fuzzy-Based Taguchi Method." *Materials & Manufacturing Processes*, Vol. 18(2), 2003, pp. 229.

21. Zhang, L., "An Investigation of Material Removal in Polishing with Fixed Abrasives." *Proceedings of the Institution of Mechanical Engineers, Part B: Journal of Engineering Manufacture*, Vol. 216, 2002, pp. 103-112.

22. Lin, T. R., "The Use of Reliability in the Taguchi Method for the Optimisation of the Polishing Ceramic Gauge Block." *The International Journal of Advanced Manufacturing Technology*, Vol. 22(3-4), 2003, pp. 237-242.

23. Liu, C. W., "Modeling of the Wear Mechanism During Chemical-mechanical Polishing." *Journal of the Electrochemical Society*, Vol. 143(2), 1996, pp. 716-721.

24. Yuan, J. L., "Research on Abrasives in the Chemical-mechanical Polishing Process for Silicon Nitride Balls." *Journal of Materials Processing Technology*, Vol. 129(1-3), 2002, pp. 171-175.

25. Wang, Y. G., Zhang, L.C., and Biddut, A., "Chemical Effect on the Material Removal Rate in the CMP of Silicon Wafers." *Wear*, Vol. 270(3-4), 2011, pp. 312-316.

26. Oh, S., "An Integrated Material Removal Model for Silicon Dioxide Layers in Chemical Mechanical Polishing Processes." *Wear*, Vol. 266(7-8), 2009, pp. 839-849.

27. Tseng, W. T., "Comparative Study on the Roles of Velocity in the Material Removal Rate During Chemical Mechanical Polishing." *Journal of the Electrochemical Society*, Vol. 146(5), 1999, pp. 1952-1959.

28. Uhlmann, E., "Influence of Kinematics on the Face Grinding Process on Lapping Machines." *CIRP Annals*, Vol. 48, 1999, pp. 281-284.

29. Wrschka, P., "Polishing Parameter Dependencies and Surface Oxidation of Chemical Mechanical Polishing of Al Thin Films." *Journal of the Electrochemical Society*, Vol. 146(7), 1999, pp. 2689-2696.

30. Touge, M., Watanabe, J., and Matsuo, T., "Ultra-thinning Processing of Dielectric Substrates by Precision Abrasive Machining." *CIRP Annals - Manufacturing Technology*, Vol. 55, 2006, pp. 317-320.

31. Chang, K. Y., Song, Y. H., and Lin, T. R., "Analysis of Lapping and Polishing of a Gauge Block." *The International Journal of Advanced Manufacturing Technology*, Vol. 20(6), 2002, pp. 414-419.

32. Chauhan, R., "Role of Indentation Fracture in Free Abrasive Machining of Ceramics." *Wear*, Vol. 162-164, 1993, pp. 246-257.

33. Preston, F., "The Theory and Design of Plate Glass Polishing Machines." *Society of Glass Technology*, Vol. 11, 1927, pp. 214-256.

34. Buijs, M., "Three-body Abrasion of Brittle Materials as Studied by Lapping." *Wear*, Vol. 166(2), 1993, pp. 237-245.

35. Buijs, M., "A Model for Lapping of Glass." *Journal of Materials Science*, Vol. 28(11), 1993, pp. 3014-3020.

36. Moore, M.A., "Abrasive Wear of Brittle Solids.". *Wear*, Vol. 60, 1980, pp. 123-140.

37. llez-Arriaga, L. and Téllez, A., "Correction of the Preston Equation for Low Speeds." *Applied Optics*, Vol. 46(9), pp. 1408-1410.

38. Le, X., "Statistical Description of Preston's Coefficient for Loose Abrasive Processes." *Machining Science and Technology*, Vol. 4, 2000 pp. 59-80.

39. Le, X. and Peterson, M. L., "Material Removal Rate in Flat Lapping." *Journal of Manufacturing Processes*, Vol. 1, 1999, pp. 71-78.

40. Pritchard, C., "Role of the Lubricant in Three-body Abrasion." *Nature*, Vol. 256(5244), 1970, pp. 446-447.

41. Miller, N.E., "Three-body Abrasive Wear with Small Size Diamond Abrasives." *Wear*, Vol. 58(2), 1980, pp. 249-259.

42. Chuang, H. C., "An Investigation of Lapping Characteristics for Improving the Form Error of an Aspheric Lens." *Journal of Materials Processing Technology*, Vol. 176(1-3), 2006, pp. 183-190.

43. Rabinowicz, E., "A Study of Abrasive Wear Under Three-Body Conditions." *Wear*, Vol. 4, 1961, pp. 345-355.

44. Rabinowicz, E., "Effect of Abrasive Particle Size on Wear." *Wear*, Vol. 8, 1965, pp. 381-390.

45. Wen, D., "Experimental Investigation on the Effect of Abrasive Grain Size on the Lapping Uniformity of Sapphire Wafer." *Proceedings of SPIE,* Bellingham, WA, 2009, International Society for Optical Engineering, pp. 72820C1-6.

46. Tsann-Rong, L. and Chin-Ru, S., "Experimental Study of Lapping and Electropolishing of Tungsten Carbides." *International Journal of Advanced Manufacturing Technology*, Vol. 36(7-8), 2008, pp. 715-723.

47. Deshpande, L. S., "Observations in the Flat Lapping of Stainless Steel and Bronze." *Wear*, Vol. 256(1-2), 2008, pp. 105-116.

48. Filho, J.M.C. and Crichingo, F., "An Investigation of Acoustic Emission to Monitoring Flat Lapping with Non-replenished Slurry." *The International Journal of Advanced Manufacturing Technology*, Vol. 33(7-8), 2007, pp. 730-737.

49. Sankar, M., "Experimental Investigations into Rotating Workpiece Abrasive Flow Finishing." *Wear*, Vol. 267(1-4), 2009, pp. 43-51.

50. Yuan, J. L., "Research and Simulation on the Wear Uniformity of Lapping Plate." *Key Engineering Materials*, Vol. 364-366, 2007, pp. 466-469.

51. Wang, W., Gao, P., and Wen, D., "Theoretical Analysis and Uniformity of Trajectories in Lapping Process." *Advanced Materials Research*, Vol. 102-104, 2010, pp. 625-629.

52. Kling, J. and Matthias, E., "Workpiece Material Removal and Lapping Wheel Wear in Plane and Plane-Parallel Lapping." *CIRP Annals - Manufacturing Technology*, Vol. 35, 1986, pp. 219-222.

53. Fang, A., "Influence of Kinematics on Lapping Efficiency and Lap Wear." *Society of Manufacturing Engineers*, Vol. 38, 2010, pp. 153-160.

54. Sanchez, L.E.A., "Surface Finishing of Flat Pieces When Submitted to Lapping Kinematics on Abrasive Disc Dressed Under Several Overlap Factors." *Precision Engineering*, Vol. 35(2), 2011, pp. 355-363.

APPENDIX A

The following figures are quantile, box-whisker, and density plots from test procedures that were run.

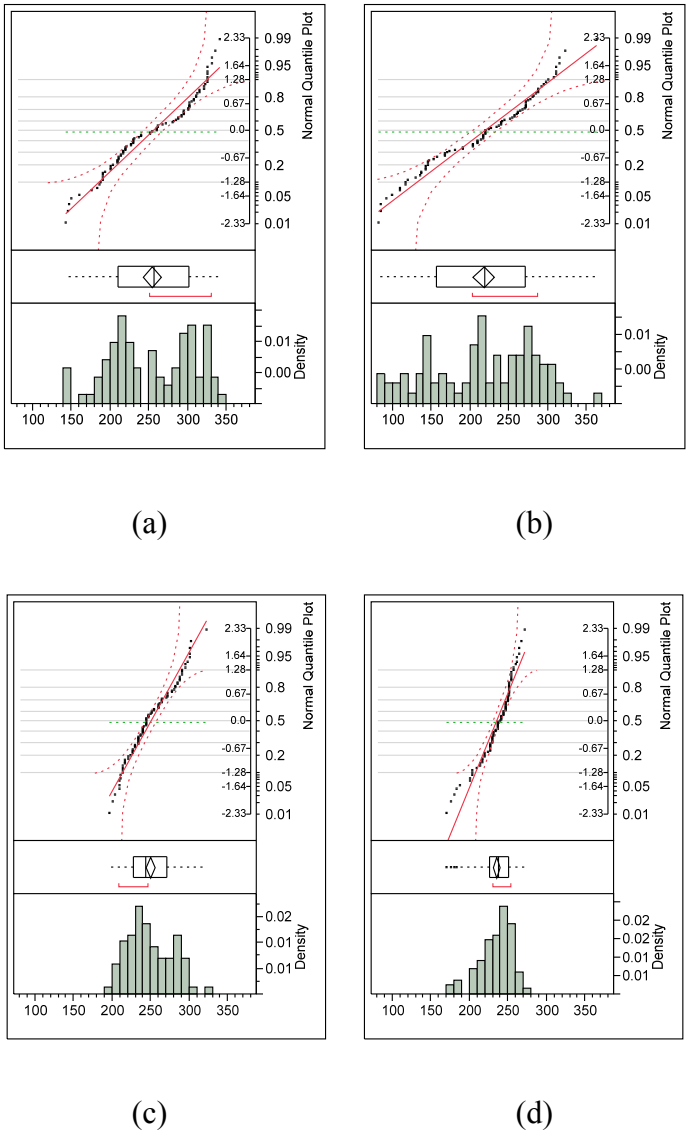

Figure 41. Quantile, box-wisker, and density plot of MRR results from sample holder made out of nitrile rubber with a hardness of (a) 10A (b) 20A (c) 30A (d) 40A

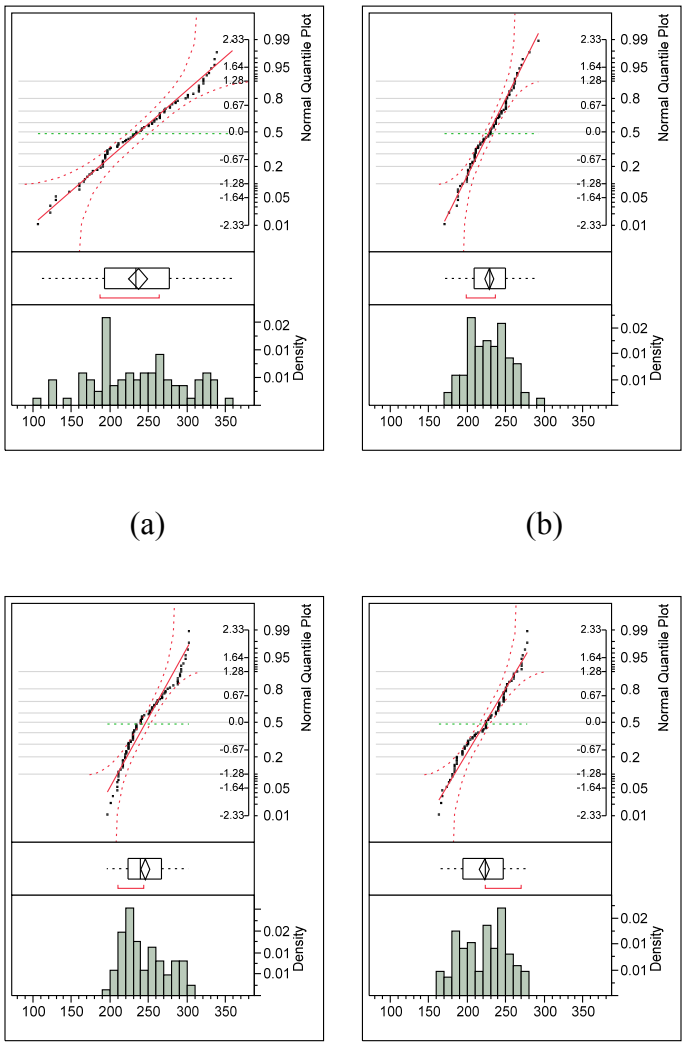

Figure 42. Quantile, box-wisker, and density plot of MRR results from sample holder made out of nitrile rubber with a hardness of (a) 50A (b) 60A (c) 70A (d) 80A

APPENDIX B

The following tables give p-values based on Student's t-tests at 95% confidence intervals. The tables are labeled with references to the corresponding data set that they are from.

Table 31. P-values from a student's t-test from results shown in Figure 18

Test 1	Test 2	p-Value	Test 1	Test 2	p-Value	Test 1	Test 2	p-Value
.111%, 100g/L	.133%, 125g/L	<.0001	.111%, 125g/L	.133%, 125g/L	<.0001	.111%, 75g/L	.133%, 100g/L	0.1076
.111%, 100g/L	.133%, 100g/L	<.0001	.111%, 100g/L	.111%, 75g/L	<.0001	.133%, 75g/L	.111%, 125g/L	0.2174
.133%, 75g/L	.133%, 125g/L	<.0001	.111%, 100g/L	.133%, 75g/L	0.0002	.111%, 75g/L	.111%, 125g/L	0.3586
.111%, 75g/L	.133%, 125g/L	<.0001	.133%, 100g/L	.133%, 125g/L	0.0003	.111%, 125g/L	.133%, 100g/L	0.4848
.111%, 100g/L	.111%, 125g/L	<.0001	.133%, 75g/L	.133%, 100g/L	0.0549	.133%, 75g/L	.111%, 75g/L	0.7504

Table 32. P-values from a student's t-test from results shown in Figure 19

Test 1	Test 2	p-Value
0.133% Carbomer	Water	<.0001
0.111% Carbomer	Water	<.0001
0.133% Carbomer	0.111% Carbomer	0.7841

Table 33. P-values from a student's t-test from results shown in Figure 21

Test 1	Test 2	p-Value
140/170 mesh	106-125 microns	<.0001
140/170 mesh	90-106 microns	0.0003
90-106 microns	106-125 microns	0.0066

Table 34. P-values from a student's t-test from results shown in Figure 22

Test 1	Test 2	p-Value	Test 1	Test 2	p-Value	Test 1	Test 2	p-Value
43.4 KPa, 100 g/L	33.6 KPa, 75 g/L	<.0001	43.4 KPa, 100 g/L	56.0 KPa, 100 g/L	0.0002	43.4 KPa, 75 g/L	33.6 KPa, 75 g/L	0.0823
56.0 KPa, 125 g/L	33.6 KPa, 75 g/L	<.0001	56.0 KPa, 125 g/L	56.0 KPa, 100 g/L	0.0006	43.4 KPa, 100 g/L	43.4 KPa, 125 g/L	0.3072
43.4 KPa, 125 g/L	33.6 KPa, 75 g/L	<.0001	43.4 KPa, 125 g/L	43.4 KPa, 75 g/L	0.0012	56.0 KPa, 125 g/L	43.4 KPa, 125 g/L	0.4437
43.4 KPa, 100 g/L	43.4 KPa, 75 g/L	<.0001	43.4 KPa, 125 g/L	56.0 KPa, 75 g/L	0.0014	56.0 KPa, 100 g/L	43.4 KPa, 75 g/L	0.576
43.4 KPa, 100 g/L	56.0 KPa, 75 g/L	<.0001	43.4 KPa, 125 g/L	56.0 KPa, 100 g/L	0.0067	56.0 KPa, 100 g/L	56.0 KPa, 75 g/L	0.6191
56.0 KPa, 125 g/L	43.4 KPa, 75 g/L	<.0001	56.0 KPa, 100 g/L	33.6 KPa, 75 g/L	0.0224	43.4 KPa, 100 g/L	56.0 KPa, 125 g/L	0.7976
56.0 KPa, 125 g/L	56.0 KPa, 75 g/L	<.0001	56.0 KPa, 75 g/L	33.6 KPa, 75 g/L	0.0721	56.0 KPa, 75 g/L	43.4 KPa, 75 g/L	0.9504

Table 35. P-values from a student's t-test from results shown in Figure 24

Test 1	Test 2	p-Value	Test 1	Test 2	p-Value	Test 1	Test 2	p-Value
0.111%, 3-slot	0.111 %, 12-slot	0.1089	0.133%, solid	0.111%, Solid	0.384	0.133%, 12-slot	0.111%, Solid	0.6337
0.133%, solid	0.111 %, 12-slot	0.1551	0.111%, 3-slot	0.133%, 3-slot	0.4679	0.133%, solid	0.133%, 12-slot	0.6927
0.111%, 3-slot	0.111 %, Solid	0.292	0.111%, 3-slot	0.133%, 12-slot	0.5623	0.133%, 3-slot	0.111%, Solid	0.7415
0.133%, 12-slot	0.111 %, 12-slot	0.3027	0.111%, Solid	0.111%, 12-slot	0.578	0.111%, 3-slot	0.133%, solid	0.8536
0.133%, 3-slot	0.111 %, 12-slot	0.3762	0.133%, solid	0.133%, 3-slot	0.588	0.133%, 12-slot	0.133%, 3-slot	0.8833

Table 36. P-values from a student's t-test from results shown in Figure 25

Test A	Test B	p-Value	Test A	Test B	p-Value	Test A	Test B	p-Value
Steel, 100 g/L	Nitrile Rubber, 125 g/L	<.0001	Steel, 100 g/L	Nitrile Rubber, 75 g/L	<.0001	Steel, 100 g/L	Steel, 75 g/L	<.0001
Steel, 125 g/L	Nitrile Rubber, 125 g/L	<.0001	Steel, 125 g/L	Nitrile Rubber, 75 g/L	<.0001	Steel, 125 g/L	Steel, 75 g/L	<.0001
Steel, 100 g/L	Nitrile Rubber, 100 g/L	<.0001	Steel, 75 g/L	Nitrile Rubber, 100 g/L	<.0001	Nitrile Rubber, 100 g/L	Nitrile Rubber, 125 g/L	<.0001
Steel, 125 g/L	Nitrile Rubber, 100 g/L	<.0001	Steel, 75 g/L	Nitrile Rubber, 75 g/L	<.0001	Nitrile Rubber, 75 g/L	Nitrile Rubber, 100 g/L	0.0011
Steel, 75 g/L	Nitrile Rubber, 125 g/L	<.0001	Nitrile Rubber, 75 g/L	Nitrile Rubber, 125 g/L	<.0001	Steel, 100 g/L	Steel, 125 g/L	0.0327

Table 37. P-values from a student's t-test from results shown in Figure 29

Test 1	Test 2	p-Value
30 mL/min, 116.67 g/L	30 mL/min, 75 g/L	<.0001
46.67 mL/min, 75 g/L	30 mL/min, 75 g/L	<.0001
30 mL/min, 116.67 g/L	46.67 mL/min, 75 g/L	0.0053

VITA

Jason Michael Sowers received his Bachelor of Science degree in mechanical engineering from Texas A&M University in May 2009. He began his Master of Science degree for mechanical engineering at Texas A&M University in August 2009 and graduated in August 2011. His main interests in research are on abrasive machining processes and more specifically lapping.

Mr. Sowers may be reached through his Master's Thesis advisor, Dr. Hong Liang, at Texas A&M University, Department of Mechanical Engineering, 3123 TAMU, College Station, TX 77845-3123. His email address is jmsowers@gmail.com.